

AD-A049 547

POLYTECHNIC INST OF NEW YORK BROOKLYN DEPT OF ELECTR--ETC F/G 20/9
STUDIES OF PARAMETRIC DECAY INSTABILITIES IN MAGNETO PLASMAS. (U)

JUN 77 S KUO, B R CHEO

AFOSR-74-2668

UNCLASSIFIED

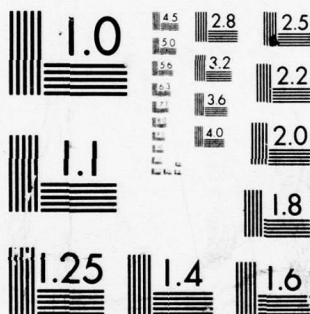
POLY-EE/EP-77-207

AFOSR-TR-78-0033

NL

1 OF 1
AD
A049547





MICROCOPY RESOLUTION TEST CHART
NATIONAL BUREAU OF STANDARDS-1963-A

Polytechnic Institute of New York

Department of
Electrical Engineering

(2)
SC

SCIENTIFIC REPORT

STUDIES OF PARAMETRIC DECAY INSTABILITIES

IN MAGNETO PLASMAS

June 1977

for

Air Force Office of Scientific Research

under

Grant No. AFOSR-74-2668
Project No. 9751-03

Submitted by

Szu-Ping Kuo
Bernard R-S Cheo

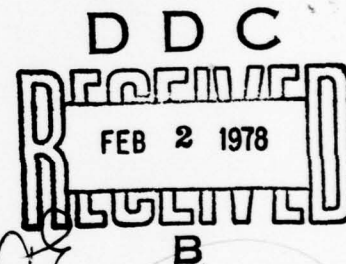
Report No. POLY EE/EP 77-027

Reproduction in whole or in part is permitted
for any purposes of the United States Government.

Approved for public release; distribution unlimited.

DEPARTMENT OF ELECTRICAL ENGINEERING AND ELECTROPHYSICS

POLYTECHNIC INSTITUTE OF NEW YORK



SCIENTIFIC REPORT

STUDIES OF PARAMETRIC DECAY INSTABILITIES
IN MAGNETO PLASMAS

June 1977

for

Air Force Office of Scientific Research
Arlington, Virginia

under

Grant No. AFOSR-74-2668
Project No. 9751-03

Submitted by

Szu-Ping Kuo
Bernard R-S Cheo

Report No. POLY EE/EP 77-027

Reproduction in whole or in part is permitted
for any purposes of the United States Government.

Approved for public release; distribution unlimited.

DEPARTMENT OF ELECTRICAL ENGINEERING AND ELECTROPHYSICS

POLYTECHNIC INSTITUTE OF NEW YORK

AIR FORCE OFFICE OF SCIENTIFIC RESEARCH (AFSC)
NOTICE OF TRANSMITTAL TO DDC
This technical report has been reviewed and is
approved for public release IAW AFR 190-12 (7b).
Distribution is unlimited.
A. D. BLOSE
Technical Information Officer

ABSTRACT

A theory is developed for the parametric excitation of coupled waves in a uniform magneto plasma. Instead of using electrostatic approximation which is valid only for longitudinal waves, a general formulation of the parametric coupling equations is developed by using Hamiltonian approach. The plasma is pumped by a monochromatic electromagnetic wave with frequency ω_0 which decays into two decay waves ω_l and ω_s (e.g., a plasmon and a phonon) with $\omega_0 = \omega_l + \omega_s$. Either one of the plasma modes coupled with the pump wave (through the linearized Vlasov equation) to induce a polarization which may act as the source of another mode. A general procedure to calculate the induced polarizations is introduced by transforming the linearized Vlasov equation into the oscillating frame of reference, in which the equation can then be solved by the method of characteristics. The threshold power, initial growth rate and the frequency shift (due to finite initial growth rate) of the parametric instabilities can be obtained from the coupled mode equations and the results obtained can be applied to all the wavelength region. Several interesting cases are presented and compared favorably with experiments.

The simultaneous excitation of second harmonic of electron-cyclotron and electrostatic ion-cyclotron oscillations by means of a monochromatic electromagnetic wave at $\omega_0 = 9.23$ GHz has been observed experimentally. The experiment has been conducted in a microwave sustained beam plasma. By switching the pump power between two levels, the time evolution of the excited electrostatic ion-cyclotron wave is studied. In order to explain the observed nonlinear saturated state of the instability, the nonlinear damping rate due to two possible mechanisms has been examined. Harmonic generation gives very small contributions, therefore, anomalous diffusion caused

by the coherent oscillation of the electrostatic ion-cyclotron wave plays an important role. Working in the guiding center frame, the effective non-linear damping frequency pertaining to the diffusion process is obtained.

ACCESSION for		
NTIS	White Section	<input checked="" type="checkbox"/>
DDC	Buff Section	<input type="checkbox"/>
UNANNOUNCED		<input type="checkbox"/>
JUSTIFICATION _____		
BY _____		
DISTRIBUTION/AVAILABILITY CODES		
Dist.	AVAIL.	and/or SP. CIAL
A		

TABLE OF CONTENTS

	<u>Page</u>
ABSTRACT	ii
LIST OF FIGURES	vi
LIST OF TABLES	vii
I. INTRODUCTION	1
II. GENERAL FORMULATION FOR THE PARAMETRIC EXCITATION	6
1. Overall Physical Features	6
2. Hamiltonian Approach	6
III. KINETIC APPROACH TO CALCULATE THE COUPLING COEFFICIENTS	12
1. Transformation of the Vlasov Equations to the Oscillating Frame of Reference	12
2. Integration Along the Unperturbed Trajectory in the Phase Space	14
IV. DETAILED ANALYSIS OF THRESHOLD POWER AND INITIAL GROWTH RATE	23
1. Conditions and Properties of the Instabilities Occuring on the Basis of a General Form of the Coupled Mode Equations	23
2. Parametric Decay into Longitudinal Modes (Electrostatic Approximation)	26
3. Parametric Decay into Electrostatic Ion Cyclotron Wave and Harmonics of Electron Cyclotron Wave (Hybrid Mode) in a Uniform Magneto Plasma	33
4. Comparison Between Theory and Experiments	36
V. DESCRIPTION OF EXPERIMENT AND RESULTS	38
1. Experimental Apparatus and Procedure	38
2. Measurement of Growth and Decay Times of Electrostatic Ion Cyclotron Waves	43
3. Frequency of Electrostatic Ion Cyclotron Wave as a Function of Pump Power	55
4. Summary of Experimental Parameters	60
5. Evidence of Parametric Excitation of Electrostatic Ion Cyclotron Wave	61
6. Simplified Theoretical Explanation	66
VI. NONLINEAR SATURATION MECHANISM	66
1. Introduction	66
2. Theory	67
3. Comparison between Theory and Experimental Results	73

TABLE OF CONTENTS (continued)

	<u>Page</u>
VII. CONCLUSIONS	75
APPENDIX A: NORMALIZATION OF THE ACOUSTIC MODES	76
APPENDIX B: NORMALIZATION OF THE OPTICAL MODES	80
REFERENCES	83

LIST OF FIGURES

	<u>Page</u>
1. Schematic Diagram of PINY HCD System	39
2. Simplified Block Diagram of Experimental Apparatus	41
3. Frequency Spectrum of Electrostatic Ion Cyclotron Wave	42
4. Time Domain Behavior of Electrostatic Ion Cyclotron Wave	42
5. Growth and Decay of Electrostatic Ion Cyclotron Waves as a Function of Pump Power	44
6. Decay and Growth of Electrostatic Ion Cyclotron Wave From One Steady State Amplitude into Another	47
7. Photograph Shows that There is a Transition Period Before Wave Really Starts to Grow	47
8. Average Decay Rate of Electrostatic Ion Cyclotron Wave as a Function of Power P_2 with $P_1=173$ W Fixed	49
9. Initial Growth Rate of Electrostatic Ion Cyclotron Wave From One Steady State Amplitude to Another as a Function of Power P_2 . $P_1=173$ W, $p=1.2\mu$, $f_o=9.23$ GHz	50
10. Decay of Electrostatic Ion Cyclotron Wave from Steady State Amplitude into Noise for Pump Power Just Below Threshold Level.	51
11. Growth and Decay of Electrostatic Ion Cyclotron Wave for $P_1=173$ W and $P_2=0$ W	54
12. Frequency of Electrostatic Ion Cyclotron Wave as a Function of Pump Power	57
13. Measured Electrostatic Ion Cyclotron Frequency Shift as a Function of Electron Temperature Change	58
14. Plasma Density as a Function of Pump Power	58
15. Square of the Saturated Amplitude of the Electrostatic Ion Cyclotron Wave as a Function of Pump Power for Power Above Threshold	63

LIST OF TABLES

	<u>Page</u>
1. Experimental and Theoretical Data in Several Pump Power Levels	56
2. Experimental Parameters	59

I. INTRODUCTION

Plasma parametric instabilities occur when the pump amplitude exceeds a threshold which depends on the set of coupled modes and on their damping effects. It has become of special interest following the recognition that such processes play important roles in the absorption of electromagnetic power¹. Experimental results showed that parametric instabilities may form a channel for efficient transfer of electromagnetic energy into a rather large size hot plasma, and the nonlinear effects of these instabilities may introduce a mechanism which heats plasma more efficiently than classical collisional absorption². Therefore, most of the experimental effort has been expended on observing the plasma heating rates. Besides plasma heating, theoretical and experimental studies of parametric decay instabilities will also yield information about the linear and nonlinear damping rates of the instabilities, and the development of plasma turbulence. In the previous report³, a detailed experimental study of the dynamics of the process had been given. Klein and Cheo^{3,24} introduce a technique for experimentally determining growth and decay characteristics of parametrically excited plasma waves. They found that the dominate linear damping mechanism of the ion acoustic wave in their plasma is due to ionization collisions, not due to ion-neutral collisions which is the usual phenomenon. Theirs is a unmagnetized plasma, while this effort is the continuation of their experimental study into a magnetoplasma. Therefore, different modes are involved. Since there are no available theories for our experiment, a general theory is also developed by using system total Hamiltonian approach to deal with the problem. Comparison with our experiment has also been made.

Indeed, the detailed ways of implementation of the ideas of parametric decay instabilities to plasma heating is still developing. Grek and Porkolab²,

Porkolab et al.⁴, and Okabayashi⁵ et al. had performed experiments by shining microwave power onto a plasma column in the extraordinary mode of propagation in the region of the upper hybrid frequency. Wavelength measurements of the decay waves showed decay into upper hybrid waves (and Bernstein waves) and lower hybrid and/or ion acoustic waves. It was shown that significant ion and electron heating occurred only above threshold for parametric instabilities. There were also several experiments^{6, 7, 8} performed in the regime of lower hybrid frequency which showed parametric decay into lower hybrid waves and ion acoustic waves, ion cyclotron waves, ion quasi modes, or drift waves may occur. Again, strong plasma heating was observed above threshold for parametric instabilities (both ion and electrons). Experimental technique to observe the plasma heating rates is by using a multigrid energy analyzer to measure the modified electron and ion distribution function. Another technique is also developing by switching the pump power between two levels and using the Fabry-Perot interferometer to measure the ion temperature growth rate.

In the parametric process, the incident pump wave is couples to two or more natural modes of the plasma by satisfying both conservation of frequency and conservation of wave vector relations. The frequency mixing allows energy supplied to the system at one frequency to be converted to another. The physical origin of mode coupling mechanism is fairly easy to understand on a qualitative basis. From linear wave analyses, the dielectric tensor of the plasma is density dependent. Hence it will be modulated by the presence of the vibrational modes of the plasma, resulting in a mixing action such that the input radiation and vibrational modes beat together to produce sum and difference frequencies. These in turn may act as sources for parametric excitations if the frequency and wave vector matching conditions

are satisfied.

By assuming $\exp(-i\omega t)$ time behavior for the mode of interest, decay or growth of the mode will be decided by the dispersion relation of the system. Therefore, most of the theoretical investigations are directed toward finding the modified dispersion relations with the presence of a pump wave in the system. The first work is done by Silin.⁹ His theory is largely based on the hydrodynamic equations for a cold plasma. DuBois and Goldman¹⁰ analyze the parametric coupling of Langmuir and ion-acoustic oscillations based on a Green's function perturbative method (harmonic approximation), which is restricted to the case when the radiation-induced energy of the particles is small compared to their thermal energy. They showed that the plasma can be unstable to certain applied frequencies for pump power above a threshold, a characteristic of parametric excitation. Later, Nishikawa,¹¹ and Lee and Su¹² used hydrodynamic model and obtained same conclusions. However, in order to justify the harmonic approximation for greater intensities, Jackson¹³ pointed out that it is important to estimate the range of frequencies which produces instabilities when the intensity is large.

Parametric coupling of electrostatic waves in a magnetized plasma have been treated by Aliev et al.,¹⁴ by Amano and Okamoto,¹⁵ and by Porkolab,^{16, 17} and others. These authors used the linearized Vlasov equation with self consistent potential field, which can be solved easily after transformation to the oscillating frame of reference. Alieve et al. found the frequency range of a pump wave in which the plasma is unstable turns out to be much broader than in the case of a unmagnetized plasma. Amano and Okamoto extend the theory to inhomogeneous cases. Porkolab analyzed the resulting dispersion relation of Aliev et al. in the limit of

weak coupling, and obtained threshold powers to excite the upper and lower hybrid (or ion acoustic) modes simultaneously. He also introduced a new type of kinetic-dissipative instability. All of the above investigations are based on electrostatic approximation for the plasma modes and hence valid only for longitudinal waves. In the presence of a static magnetic field, most of the plasma modes become hybrid, and the electrostatic approximation holds only in the limiting case.

In this investigation a general formulation of the parametric coupling equations in a homogeneous magnetized plasma is developed by using Hamiltonian approach.¹⁸ The coupling coefficients of the parametric equations are derived from the collisionless Boltzman-Vlasov equation. With transformation method and trajectory techniques, the induced polarization currents are derived. Applications to various forms of modal coupling are given, and comparison with experimental works is made whenever possible.

A set of experiments in the Poly HCD plasma was performed. A microwave horn is mounted at the end of the plasma beam. In order to obtain a quiescent plasma, a new technique to create an ultrastable microwave sustained plasma is introduced. When the pump signal, at 9.23 GHz, is above the threshold level, the second harmonics of the electron cyclotron wave and the electrostatic ion-cyclotron wave are simultaneously excited. The time evolution process of the electrostatic ion-cyclotron wave is studied by switching the microwave pump power from one level to another. Linear damping rate, initial growth rate, and the threshold power can be obtained.

In addition, the nonlinear saturation mechanisms observed in the experiment are discussed. An analysis by using the guiding center

technique¹⁸ was made and it is established the nonlinear damping is due to the anomalous diffusion produced by the ponderomotive forces of the instabilities. Comparison with experiments is favorable.

II. GENERAL FORMULATION FOR THE PARAMETRIC EXCITATION

1. Overall Physical Features

It is well known that the vibrational modes of a medium will modulate the permittivity or polarizability of the medium. Assume that there exist two normal modes or waves, S and L (e. g., a phonon and a plasmon) in the medium with frequencies ω_s and ω_l in the linear regime; then they will modulate the polarizability of the medium resulting from the density perturbation of the medium. The problem can be treated mathematically by expanding the electrostrictive polarizability α_{ij} in a Taylor's series in terms of normal mode vibrational field $\delta \underline{E}_s$ related to S and $\delta \underline{E}_l$ related to L

$$\therefore \alpha_{ij} = \alpha_{ij}^0 + \left(\frac{\partial \alpha_{ij}}{\partial \delta \underline{E}_{s\sigma}} \right)_0 \delta E_{s\sigma} + \left(\frac{\partial \alpha_{ij}}{\partial \delta \underline{E}_{l\sigma}} \right)_0 \delta E_{l\sigma} \quad \text{where } i, j, \sigma = 1, 2, 3 \text{ or } x, y, z$$

where the Einstein summation convention is understood. Hence the total induced polarization due to the presence of a third wave field \underline{E} is

$$P_i^t = \alpha_{ij} E_j = \left[\alpha_{ij}^0 + \left(\frac{\partial \alpha_{ij}}{\partial \delta \underline{E}_{s\sigma}} \right)_0 \delta E_{s\sigma} + \left(\frac{\partial \alpha_{ij}}{\partial \delta \underline{E}_{l\sigma}} \right)_0 \delta E_{l\sigma} \right] E_j = P_i^0 + \delta P_i + \delta \mathcal{P}_i$$

where $\delta P_i = \left(\frac{\partial \alpha_{ij}}{\partial \delta \underline{E}_{s\sigma}} \right)_0 \delta E_{s\sigma} E_j$ and $\delta \mathcal{P}_i = \left(\frac{\partial \alpha_{ij}}{\partial \delta \underline{E}_{l\sigma}} \right)_0 \delta E_{l\sigma} E_j$ are the induced polarization associated with the Raman and Brillouin effects. Here we have assumed $|\underline{E}| \gg |\delta \underline{E}_s|$ and $|\underline{E}| \gg |\delta \underline{E}_l|$.

2. Hamiltonian Approach

We first normalize both S and L waves. Assume the particles associated with S and L have reduced masses M and m, momentum K and \mathcal{K} , displacements Q and U respectively. The displacement and

momentum variables are the canonical conjugate pairs. Hence the unperturbed Hamiltonian density $H_{os}^{(k)}$ and $H_{ol}^{(k)}$ are

$$H_{os}^{(k)} = \frac{1}{2} \sum_{\sigma} \left[\frac{K_{\sigma}^2(k)}{M} + M \omega_s'^2(k) Q_{\sigma}^2(k) \right] \quad (2.1)$$

$$H_{ol}^{(k)} = \frac{1}{2} \sum_{\sigma} \left[\frac{\mathcal{K}_{\sigma}^2(k)}{m} + m \omega_l'^2(k) U_{\sigma}^2(k) \right] \quad (2.2)$$

where $\omega_s'(k)$ and $\omega_l'(k)$ are the resonant frequencies of the system without the pump field, and the field associated with the corresponding modes are

$$\delta \underline{E}_s(k) = - \frac{M}{e} \frac{1}{\sqrt{n_0}} \omega_s^2(k) \underline{Q}(k) - \frac{\Omega_i}{e \sqrt{n_0}} \underline{K}(k) \times \hat{z} \quad (2.3)$$

$$\delta \underline{E}_l(k) = \frac{m}{e} \frac{1}{\sqrt{n_0}} \omega_l^2(k) \underline{U}(k) + \frac{\Omega_e}{e \sqrt{n_0}} \underline{\mathcal{K}}(k) \times \hat{z} \quad (2.4)$$

where $\omega_s(k)$ and $\omega_l(k)$ are the resonant frequencies with the presence of pump field. n_0 is the background electron (or ion) density. Ω_e and Ω_i are cyclotron frequencies of the two species including the sign of the charge. Here we also assume that a uniform magnetic field $B_0 \hat{z}$ is applied, and the plasma is singly ionized. It is easy to show that the Poisson bracket relations hold:

$$\{ Q_{\sigma}(k) , K_{\beta}(k') \} = \delta(k, k') \delta_{\sigma\beta} \quad (2.5)$$

$$\{ U_{\sigma}(k) , \mathcal{K}_{\beta}(k') \} = \delta(k, k') \delta_{\sigma\beta} \quad (2.6)$$

The pump field is assumed to be spatially homogeneous (dipole approximation). Hence the induced polarizations corresponding to the frequency

components in question can be expressed as

$$\delta P_{si}^{(k)} = \left(\frac{\partial \alpha_{ij}}{\partial \delta E_{l\sigma}^+(k)} \right)_0 \delta E_{l\sigma}^+(k) E_j^- + c. c. \quad (2.7)$$

$$\delta P_{li}^{(k)} = \left(\frac{\partial \alpha_{ij}}{\partial \delta E_{s\sigma}^-(k)} \right)_0 \delta E_{s\sigma}^-(k) E_j^+ + c. c. \quad (2.8)$$

where the superscripts "+" denote respectively $\exp(+i\omega t)$. Then the interaction Hamiltonian densities for S and L are

$$H_s'^{(k)} = -\delta P_{si}^{(k)} \delta E_{si}^{(k)} = \delta P_{si}^{(k)} \left[\frac{M}{e} \frac{1}{\sqrt{n_0}} \omega_s^2(k) Q_i(k) + \frac{\Omega_i}{e \sqrt{n_0}} (K(k) \times \hat{z})_i \right] \quad (2.9)$$

$$H_l'^{(k)} = -\delta P_{li}^{(k)} \delta E_{li}^{(k)} = -\delta P_{li}^{(k)} \left[\frac{m}{e} \frac{1}{\sqrt{n_0}} \omega_l^2(k) U_i(k) + \frac{\Omega_e}{e \sqrt{n_0}} (M(k) \times \hat{z})_i \right] \quad (2.10)$$

The total Hamiltonian densities of the S and L are

$$H_s^{(k)} = H_{os}^{(k)} + H_s'^{(k)} \quad (2.11)$$

$$H_l^{(k)} = H_{ol}^{(k)} + H_l'^{(k)} \quad (2.12)$$

It is known in general that the equation of motion for any cononical variable A is

$$\left[\frac{d^2}{dt^2} + 2\Gamma \frac{d}{dt} + \Gamma^2 \right] A = \{ \{A, H\}, H \} \quad (2.13)$$

where $1/\Gamma$ is the phenomenological relaxation time, and H is the total Hamiltonian density. (2.13) together with (2.1) to (2.12) can be used to

derive the coupled mode equations:

Evaluation of the Poisson bracket $\{ \{Q_i(\underline{k}), H_s^{(k)}\} , H_s^{(k)} \}$ with the aid of (2.1), (2.5), (2.9) and (2.11) yields

$$\{ \{Q_i(\underline{k}), H_s^{(k)}\} , H_s^{(k)} \} = -\omega_s'^2(\underline{k}) Q_i(\underline{k}) - \frac{\omega_s^2(\underline{k})}{e\sqrt{n_0}} \delta P_{si}^{(k)}$$

Therefore the appropriate equation of motion for $Q_i(\underline{k})$ is given by (2.13),

$$\ddot{Q}_i(\underline{k}) + 2\Gamma_s \dot{Q}_i(\underline{k}) + (\Gamma_s^2 + \omega_s'^2(\underline{k})) Q_i(\underline{k}) = -\frac{\omega_s^2(\underline{k})}{e\sqrt{n_0}} \delta P_{si}^{(k)} \quad (2.14)$$

with the dot denoting $\frac{d}{dt}$.

Similarly by evaluating $\{ \{K_i(\underline{k}), H_s^{(k)}\} , H_s^{(k)} \}$ with the aid of (2.1), (2.5), (2.9) and (2.11) we have:

$$\{ \{K_i(\underline{k}), H_s^{(k)}\} , H_s^{(k)} \} = -\omega_s'^2(\underline{k}) K_i(\underline{k}) - M\omega_s'^2(\underline{k}) \frac{\Omega_i}{e\sqrt{n_0}} (\hat{z} \times \delta \underline{P}_s^{(k)})_i$$

and

$$\ddot{K}_i(\underline{k}) + 2\Gamma_s \dot{K}_i(\underline{k}) + (\Gamma_s^2 + \omega_s'^2(\underline{k})) K_i(\underline{k}) = -M\omega_s'^2(\underline{k}) \frac{\Omega_i}{e\sqrt{n_0}} (\hat{z} \times \delta \underline{P}_s^{(k)})_i \quad (2.15)$$

Equation of motion in the variable $\delta \underline{E}_s(\underline{k})$ can be obtained by combining (2.14) and (2.15) with the aid of the relation (2.3). The result is

$$\left[\frac{d^2}{dt^2} + 2\Gamma_s \frac{d}{dt} + (\Gamma_s^2 + \omega_s'^2(\underline{k})) \right] \delta \underline{E}_s(\underline{k}) = \frac{M\omega_s^4(\underline{k})}{n_0 e^2} \delta \underline{P}_s^{(k)} + \frac{M\omega_s'^2(\underline{k}) \Omega_i^2}{n_0 e^2} (\hat{z} \times \delta \underline{P}_s^{(k)})_{x\hat{z}} \quad (2.16)$$

Similarly for the L mode we obtain:

$$\left[\frac{d^2}{dt^2} + 2\Gamma_l \frac{d}{dt} + (\Gamma_l^2 + \omega_l'^2(\underline{k})) \right] \delta \underline{E}_l(\underline{k}) = \frac{m\omega_l^4(\underline{k})}{n_0 e^2} \delta \underline{P}_l(\underline{k}) + \frac{m\omega_l'^2(\underline{k})\Omega_i^2}{n_0 e^2} (\hat{z} \times \delta \underline{P}_l(\underline{k})) \times \hat{z} \quad (2.17)$$

Thus, we get two coupled wave equations for S and L modes with the presence of the third wave \underline{E} . When the pump power is near or above threshold level, collisionless model can be used to calculate the coupling coefficients and replace $\Gamma_s^2 + \omega_s'^2(\underline{k})$ and $\Gamma_l^2 + \omega_l'^2(\underline{k})$ by the shifted resonant frequencies. Then equations (2.16) and (2.17) become

$$\left[\frac{d^2}{dt^2} + 2\Gamma_s \frac{d}{dt} + \omega_s^2(\underline{k}) \right] \delta \underline{E}_s(\underline{k}) = \frac{M\omega_s^4(\underline{k})}{n_0 e^2} \delta \underline{P}_s(\underline{k}) + \frac{M\omega_s'^2(\underline{k})\Omega_i^2}{n_0 e^2} (\hat{z} \times \delta \underline{P}_s(\underline{k})) \times \hat{z} \quad (2.18)$$

$$\left[\frac{d^2}{dt^2} + 2\Gamma_l \frac{d}{dt} + \omega_l^2(\underline{k}) \right] \delta \underline{E}_l(\underline{k}) = \frac{m\omega_l^4(\underline{k})}{n_0 e^2} \delta \underline{P}_l(\underline{k}) + \frac{m\omega_l'^2(\underline{k})\Omega_i^2}{n_0 e^2} (\hat{z} \times \delta \underline{P}_l(\underline{k})) \times \hat{z} \quad (2.19)$$

where $\omega_s^2(\underline{k}) = \Gamma_s^2 + \omega_s'^2(\underline{k})$, $\omega_l^2(\underline{k}) = \Gamma_l^2 + \omega_l'^2(\underline{k})$

Using the following relations

$$\delta \underline{E}_s(\underline{k}) = \delta \underline{E}_s^-(\underline{k}) + \text{c. c.} \quad \delta \underline{P}_s(\underline{k}) = \delta \underline{P}_s^-(\underline{k}) + \text{c. c.}$$

$$\delta \underline{E}_l(\underline{k}) = \delta \underline{E}_l^+(\underline{k}) + \text{c. c.} \quad \delta \underline{P}_l(\underline{k}) = \delta \underline{P}_l^+(\underline{k}) + \text{c. c.}$$

and combining the relevant components, equations (2.18) and (2.19) can be rewritten as

$$\left[\frac{d^2}{dt^2} + 2\Gamma_s \frac{d}{dt} + \omega_s^2(\underline{k}) \right] \delta \underline{E}_s^-(\underline{k}) = \frac{M\omega_s^4(\underline{k})}{n_0 e^2} \delta \underline{P}_s^-(\underline{k}) + \frac{M\omega_s'^2(\underline{k})\Omega_i^2}{n_0 e^2} (\hat{z} \times \delta \underline{P}_s^-(\underline{k})) \times \hat{z} \quad (2.20)$$

$$\left[\frac{d^2}{dt^2} + 2\Gamma_l \frac{d}{dt} + \omega_l^2(\underline{k}) \right] \delta \underline{E}_l^+(\underline{k}) = \frac{m \omega_l^4(\underline{k})}{n_o e^2} \delta \underline{P}_l^+(\underline{k}) + \frac{m \omega_l'^2(\underline{k}) \Omega_e^2}{n_o e^2} (\hat{z} \times \delta \underline{P}_l^+(\underline{k})) \times \hat{z} \quad (2.21)$$

Here (2.20) and (2.21) fit the standard form of parametric coupled wave equations with $\delta \underline{P}$ remaining formal, which is to be derived in the next section.

III. KINETIC APPROACH TO CALCULATE THE COUPLING COEFFICIENTS

1. Transformation of the Vlasov Equations to the Oscillating Frame of Reference

To derive the coupling coefficients $(\frac{\partial \alpha_{ij}}{\partial \delta E_{l\sigma}})_0$ and $(\frac{\partial \alpha_{ij}}{\partial \delta E_{s\sigma}})_0$ for determining $\delta \underline{P}$, we start from Vlasov equation for a homogeneous background distribution function $f_{\alpha}^{(0)}$:

$$\frac{\partial f_{\alpha}^{(0)}}{\partial t} + \frac{e}{m_{\alpha}} \{ \underline{E}(t) + \frac{1}{c} \underline{v}_{\alpha} \times \underline{B}_0 \} \cdot \frac{\partial f_{\alpha}^{(0)}}{\partial \underline{v}_{\alpha}} = 0 \quad (3.1)$$

where e , m_{α} and \underline{v}_{α} are respectively the charge, mass, and velocity of a particle of species α . The corresponding solution can be written in the form

$$f_{\alpha}^{(0)}(\underline{v}_{\alpha}, t) = f_{\alpha 0}(\underline{v}_{\alpha} - \frac{e}{m_{\alpha}} \int_{-\infty}^t dt' \underline{R}_{\alpha}(t-t') \cdot \underline{E}(t'), t) = f_{\alpha 0}(\underline{v}, t) \quad (3.2)$$

where

$$\underline{R}_{\alpha}(t) = \begin{bmatrix} \cos \Omega_{\alpha} t & \sin \Omega_{\alpha} t & 0 \\ \sin \Omega_{\alpha} t & \cos \Omega_{\alpha} t & 0 \\ 0 & 0 & 1 \end{bmatrix} \quad (3.3)$$

$$\Omega_{\alpha} = \frac{e}{m_{\alpha}} \frac{\beta_0}{c}$$

$$\underline{v} = \underline{v}_{\alpha} - \frac{e}{m_{\alpha}} \int_{-\infty}^t dt' \underline{R}_{\alpha}(t-t') \cdot \underline{E}(t') \quad (3.4)$$

Hence in the oscillating frame equation (3.1) reduces to

$$\frac{\partial f_{\alpha 0}(\underline{v}, t)}{\partial t} + \frac{e}{m_{\alpha}} \frac{1}{c} \underline{v} \times \underline{B}_i \cdot \frac{\partial f_{\alpha 0}(\underline{v}, t)}{\partial \underline{v}} = 0 \quad (3.5)$$

Since any function of $[\underline{v}]$ satisfies (3.5), therefore, let's assume

$f_{\alpha 0}(\underline{v}, t) = f_{\alpha 0}(\underline{v}_{||}, \underline{v}_{\perp})$, a Maxwellian distribution.

It can be shown easily that to the first order equation for the perturbative distribution function $\delta f_{\alpha}(\underline{v}_{\alpha}, \underline{r}_{\alpha}, t)$ is

$$\begin{aligned} \frac{\partial \delta f_{\alpha}(\underline{v}_{\alpha}, \underline{r}_{\alpha}, t)}{\partial t} + \underline{v}_{\alpha} \cdot \frac{\partial \delta f_{\alpha}(\underline{v}_{\alpha}, \underline{r}_{\alpha}, t)}{\partial \underline{r}_{\alpha}} + \frac{e}{m_{\alpha}} \left[\underline{E}(t) + \frac{1}{c} \underline{v}_{\alpha} \times \underline{B}_0 \right] \cdot \frac{\partial \delta f_{\alpha}(\underline{v}_{\alpha}, \underline{r}_{\alpha}, t)}{\partial \underline{v}_{\alpha}} \\ + \frac{e}{m_{\alpha}} \delta \underline{E}(\underline{r}_{\alpha}, t) \cdot \frac{\partial f_{\alpha}^{(0)}(\underline{v}_{\alpha}, t)}{\partial \underline{v}_{\alpha}} = 0 \end{aligned} \quad (3.6)$$

For convenience we transform the original variables $(\underline{v}_{\alpha}, \underline{r}_{\alpha}, t)$ to $(\underline{v}, \underline{r}, t)$ of the oscillating reference frame and introduce the function

$$\psi_{\alpha}(\underline{v}, \underline{r}, t) = \delta f_{\alpha}(\underline{v}_{\alpha}, \underline{r}_{\alpha}, t) = \delta f_{\alpha}(\underline{v} + \frac{e}{m_{\alpha}} \int_{-\infty}^t dt' \underline{R}_{\alpha}(t-t') \cdot \underline{E}(t'), \underline{r} + \underline{l}_{\alpha}, t) \quad (3.7)$$

where $\underline{r}_{\alpha} = \underline{r} + \underline{l}_{\alpha}$

$$\text{and} \quad \underline{l}_{\alpha} = \frac{e}{m_{\alpha}} \int_{-\infty}^t dt'' \underline{R}_{\alpha}(t'-t'') \cdot \underline{E}(t'') \quad (3.8)$$

with

$$\begin{aligned} \frac{\partial}{\partial t} \psi_{\alpha}(\underline{v}, \underline{r}, t) = \frac{\partial \delta f_{\alpha}(\underline{v}_{\alpha}, \underline{r}_{\alpha}, t)}{\partial t} + \frac{e}{m_{\alpha}} \left\{ \underline{E}(t') + \int_{-\infty}^t dt' \underline{R}_{\alpha}(t-t') \right\} \cdot \frac{\partial \delta f_{\alpha}(\underline{v}_{\alpha}, \underline{r}_{\alpha}, t)}{\partial \underline{v}_{\alpha}} \\ + \frac{d\underline{l}_{\alpha}}{dt} \cdot \frac{\partial \delta f_{\alpha}(\underline{v}_{\alpha}, \underline{r}_{\alpha}, t)}{\partial \underline{r}_{\alpha}} \end{aligned}$$

From (3.6), the equation for $\psi_{\alpha}(\underline{v}, \underline{r}, t)$ is then

$$\left[\frac{\partial}{\partial t} + \underline{v} \cdot \frac{\partial}{\partial \underline{r}} + \Omega_{\alpha} (\underline{v} \times \hat{z}) \cdot \frac{\partial}{\partial \underline{v}} \right] \psi_{\alpha}(\underline{v}, \underline{r}, t) = - \frac{e}{m_{\alpha}} \delta E(\underline{r} + \underline{l}_{\alpha}, t) \cdot \frac{\partial f_{\alpha 0}(\underline{v})}{\partial \underline{v}} \quad (3.9)$$

2. Integration along the unperturbed trajectory in the phase space.

Equation (3.9) can now be solved by the method of characteristics.

In this method the perturbative distribution function is calculated in the Lagrangian system of coordinates. Let's define an unperturbed trajectory of the particles as

$$\frac{d\underline{r}}{dt} = \underline{v}, \quad \frac{d\underline{v}}{dt} = \Omega_{\alpha} (\underline{v} \times \hat{z}) \quad (3.10)$$

The solution of (3.10) is

$$\underline{v}' = \underline{R}_{\alpha}(t'-t) \cdot \underline{v} \quad (3.11)$$

and

$$\underline{r}' = \underline{r} + \frac{1}{\Omega_{\alpha}} \underline{L}_{\alpha}(t'-t) \cdot \underline{v} \quad (3.12)$$

where

$$\underline{L}_{\alpha}(t) = \begin{bmatrix} \sin \Omega_{\alpha} t & 1 - \cos \Omega_{\alpha} t & 0 \\ -(1 - \cos \Omega_{\alpha} t) & \sin \Omega_{\alpha} t & 0 \\ 0 & 0 & \Omega_{\alpha} t \end{bmatrix} = \Omega_{\alpha} \int_0^t \underline{R}_{\alpha}(\tau) d\tau \quad (3.13)$$

and

$$\underline{r} = \underline{r}(t), \quad \underline{r}' = \underline{r}(t'), \quad \underline{v} = \underline{v}(t), \quad \underline{v}' = \underline{v}(t')$$

Hence along the unperturbed trajectory (3.10) equation (3.9) may be written

$$\frac{d}{dt} \psi_{\alpha}(\underline{v}, \underline{r}, t) = - \frac{e}{m_{\alpha}} \delta E(\underline{r} + \underline{l}_{\alpha}, t) \cdot \frac{\partial f_{\alpha 0}(\underline{v})}{\partial \underline{v}} \quad (3.14)$$

Substituting (3.7) in (3.14), we obtain

$$\begin{aligned} \frac{d}{dt} \delta f_{\alpha} \left(\underline{v} + \frac{e}{m_{\alpha}} \int_{-\infty}^t dt' \underline{R}_{\alpha}(t-t') \cdot \underline{E}(t') \right), \underline{r} + \underline{l}_{\alpha}, t = \\ - \frac{e}{m_{\alpha}} \delta \underline{E}(\underline{r} + \underline{l}_{\alpha}, t) \cdot \frac{\partial f_{\alpha 0}(\underline{v})}{\partial \underline{v}} \end{aligned} \quad (3.15)$$

Because of the spatial homogeneity of the background, we may assume a coordinate dependent of the non-equilibrium increment $\delta f_{\alpha} \sim e^{i \underline{k} \cdot \underline{r}_{\alpha}}$ and the perturbed field $\delta \underline{E} \sim e^{i \underline{k} \cdot \underline{r}_{\alpha}}$. Then (3.15) becomes

$$\begin{aligned} \frac{d}{dt} \delta f_{\alpha} \left(\underline{v} + \frac{e}{m_{\alpha}} \int_{-\infty}^t dt' \underline{R}_{\alpha}(t-t') \cdot \underline{E}(t'), \underline{k}, t \right) e^{i \underline{k} \cdot (\underline{r} + \underline{l}_{\alpha})} = - \frac{e}{m_{\alpha}} \delta \underline{E}(\underline{k}, t) \\ \cdot \frac{\partial f_{\alpha 0}(\underline{v})}{\partial \underline{v}} e^{i \underline{k} \cdot (\underline{r} + \underline{l}_{\alpha})} \end{aligned} \quad (3.16)$$

Let us, however, restrict ourselves to unstable (growing) solutions. We can thus invert this differentiation by integrating (3.16) with respect to time along the unperturbed particle trajectory as

$$\begin{aligned} \delta f_{\alpha} \left(\underline{v} + \frac{e}{m_{\alpha}} \int_{-\infty}^t dt' \underline{R}_{\alpha}(t-t') \cdot \underline{E}(t'), \underline{k}, t \right) = - \frac{e}{m_{\alpha}} \int_{-\infty}^t \delta \underline{E}(\underline{k}, t') \\ \cdot \frac{\partial f_{\alpha 0}(\underline{v}')}{\partial \underline{v}'} e^{i \underline{k} \cdot (\underline{r}' - \underline{r})} e^{i \underline{k} \cdot [\underline{l}_{\alpha}(t') - \underline{l}_{\alpha}(t)]} dt' \end{aligned} \quad (3.17)$$

From equation (3.12), let

$$\phi_{\alpha}(\tau) = \underline{k} \cdot (\underline{r} - \underline{r}') = - \frac{1}{\Omega_{\alpha}} \underline{k} \cdot \underline{L}_{\alpha}(-\tau) \cdot \underline{v} \quad \text{and} \quad \tau = t - t' \quad (3.18)$$

Then equation (3.17) becomes

$$\begin{aligned} \delta f_{\alpha}(\underline{v}) + \frac{e}{m_{\alpha}} \int_{-\infty}^t dt' \underline{R}_{\alpha}(t-t') \cdot \underline{E}(t'), \underline{k}, t) = - \frac{e}{m_{\alpha}} \int_0^{\infty} \delta \underline{E}(\underline{k}, t-\tau) \\ \cdot \left\{ \frac{\partial f}{\partial \underline{v}_{\perp}} \left[\cos(\Omega_{\alpha} \tau + \theta) \hat{x} + \sin(\Omega_{\alpha} \tau + \theta) \hat{y} \right] \right. \\ \left. + \frac{\partial f}{\partial v_{\parallel}} \hat{z} \right\} e^{-i\phi_{\alpha}(\tau)} e^{i\underline{k} \cdot [\underline{l}_{\alpha}(t-\tau) - \underline{l}_{\alpha}(t)]} d\tau \end{aligned} \quad (3.19)$$

where we have used following relations

$$\underline{v} = v_{\perp} \cos \theta \hat{x} + v_{\perp} \sin \theta \hat{y} + v_{\parallel} \hat{z}$$

and

$$\underline{v}' = v_{\perp} \cos(\Omega_{\alpha} \tau + \theta) \hat{x} + v_{\perp} \sin(\Omega_{\alpha} \tau + \theta) \hat{y} + v_{\parallel} \hat{z}$$

then

$$\frac{\partial f}{\partial \underline{v}'}(\underline{v}') = \frac{\partial f}{\partial \underline{v}}(\underline{v}) \left[\cos(\Omega_{\alpha} \tau + \theta) \hat{x} + \sin(\Omega_{\alpha} \tau + \theta) \hat{y} \right] + \frac{\partial f}{\partial v_{\parallel}} \hat{z}$$

Let the time dependence of the pump electric field be

$$\underline{E}(t) = 2\underline{E}_1 \sin \omega_0 t + 2\underline{E}_2 \cos \omega_0 t \quad (3.20)$$

then

$$\begin{aligned} \underline{k} \cdot [\underline{l}_{\alpha}(t-\tau) - \underline{l}_{\alpha}(t)] &= - \frac{e}{m_{\alpha}} \int_{t-\tau}^t dt' \int_{-\infty}^{t'} dt'' \underline{k} \cdot \underline{R}_{\alpha}(t'-t'') \cdot \underline{E}(t'') \\ &= (a_{\alpha 1} + b_{\alpha 2}) [\sin \omega_0 t - \sin \omega_0(t-\tau)] \\ &\quad + (a_{\alpha 2} - b_{\alpha 1}) [\cos \omega_0 t - \cos \omega_0(t-\tau)] \end{aligned} \quad (3.21)$$

and

$$\frac{e}{m_\alpha} \int_{-\infty}^t dt' \underline{R}_\alpha(t-t') \cdot \underline{E}(t') = i \frac{e}{m_\alpha} \frac{\omega_o}{\omega_o^2 - \Omega_\alpha^2} \left[\underline{A}_\alpha \cdot (\underline{E}_1^- + \underline{E}_2^-) - \underline{A}_\alpha^* \cdot (\underline{E}_1^+ + \underline{E}_2^+) \right] \quad (3.22)$$

where

$$a_{\alpha i} = 2 \frac{e}{m_\alpha} \frac{\underline{k} \cdot \underline{A}_\alpha' \cdot \underline{E}_i}{\omega_o^2 - \Omega_\alpha^2}, \quad b_{\alpha i} = 2 \frac{e}{m_\alpha} \frac{\Omega_\alpha}{\omega_o(\omega_o^2 - \Omega_\alpha^2)} \hat{z} \times \underline{k} \cdot \underline{E}_i, \quad i = 1, 2$$

and

$$\underline{A}_\alpha' = \hat{x} \hat{x} + \hat{y} \hat{y} + \frac{\omega_o^2 - \Omega_\alpha^2}{\omega_o^2} \hat{z} \hat{z} \quad (3.23)$$

and

$$\begin{aligned} \underline{E}_1^- &= i \underline{E}_1 e^{-i\omega_o t} & \underline{E}_1^+ &= -i \underline{E}_1 e^{i\omega_o t} \\ \underline{E}_2^- &= \underline{E}_2 e^{-i\omega_o t} & \underline{E}_2^+ &= \underline{E}_2 e^{i\omega_o t} \end{aligned} \quad (3.24)$$

and

$$\underline{A}_\alpha = \hat{x} \hat{x} + i \frac{\Omega_\alpha}{\omega_o} (\hat{x} \hat{y} - \hat{y} \hat{x}) + \frac{\omega_o^2 - \Omega_\alpha^2}{\omega_o^2} \hat{z} \hat{z} \quad (3.25)$$

\underline{A}_α^* is the complex conjugate of \underline{A}_α .

We may then calculate the total induced current from (3.19) as

$$\begin{aligned} \delta \underline{J}(\underline{k}, t) &= \sum_\alpha n_\alpha e_\alpha \int d\underline{v} \left[\underline{v} + \frac{e}{m_\alpha} \int_{-\infty}^t dt' \underline{R}_\alpha(t-t') \right. \\ &\quad \left. \cdot \underline{E}(t') \right] \delta f_\alpha \left(\underline{v} + \frac{e}{m_\alpha} \int_{-\infty}^t dt' \underline{R}_\alpha(t-t') \cdot \underline{E}(t'), \underline{k}, t \right) \end{aligned} \quad (3.26)$$

With the aid of (3.21) and (3.22), (3.26) becomes

$$\begin{aligned} \delta \underline{J}(k, t) = & - \sum_{\alpha} \frac{n_{\alpha} e^2}{m_{\alpha}} \int d\underline{v} \int_0^{\infty} d\tau \left\{ \underline{v} + i \frac{e}{m_{\alpha}} \frac{\omega_0}{\omega_0^2 - \Omega_{\alpha}^2} [\underline{A}_{\alpha} \cdot (\underline{E}_1^{-} + \underline{E}_2^{-}) - \underline{A}_{\alpha}^{*} \right. \\ & \cdot (\underline{E}_1^{+} + \underline{E}_2^{+}) \left. \right\} \left\{ \frac{\partial f}{\partial \underline{v}_1} \left[\cos(\Omega_{\alpha} \tau + \theta) \hat{x} + \sin(\Omega_{\alpha} \tau + \theta) \hat{y} \right] + \frac{\partial f}{\partial \underline{v}_{11}} \hat{z} \right\} \\ & \cdot \delta \underline{E}(k, t - \tau) e^{-i\phi_{\alpha}(\tau)} e^{i\{(a_{\alpha 1} + b_{\alpha 2})[\sin \omega_0 t - \sin \omega_0(t - \tau)] \\ & + (a_{\alpha 2} - b_{\alpha 1})[\cos \omega_0 t - \cos \omega_0(t - \tau)]\}} \end{aligned} \quad (3.27)$$

Since

$$\begin{aligned} & e^{i\{(a_{\alpha 1} + b_{\alpha 2})[\sin \omega_0 t - \sin \omega_0(t - \tau)] + (a_{\alpha 2} - b_{\alpha 1})[\cos \omega_0 t - \cos \omega_0(t - \tau)]\}} \\ & = \sum_{h, q=-\infty}^{+\infty} (-1)^q J_h(a_{\alpha 1} + b_{\alpha 2}) J_q(a_{\alpha 1} + b_{\alpha 2}) e^{+i(h+q)\omega_0 t - iq\omega_0 \tau} \\ & \quad + \sum_{f, g=-\infty}^{+\infty} (i)^{g-f} J_f(b_{\alpha 1} - a_{\alpha 2}) J_g(b_{\alpha 1} - a_{\alpha 2}) e^{i(f+g)\omega_0 t - ig\omega_0 \tau} \\ & \approx 1 + \frac{1}{2} [(a_{\alpha 1} + b_{\alpha 2}) - i(b_{\alpha 1} - a_{\alpha 2})] e^{i\omega_0 t} (1 - e^{-i\omega_0 \tau}) \\ & \quad - \frac{1}{2} [(a_{\alpha 1} + b_{\alpha 2}) + i(b_{\alpha 1} - a_{\alpha 2})] e^{-i\omega_0 t} (1 - e^{i\omega_0 \tau}) \end{aligned} \quad (3.28)$$

where J_n, J_q, J_f, J_g are Bessel functions and we have assumed $|a_{\alpha i}| \ll 1, |b_{\alpha i}| \ll 1$.

For the parametric interaction, we have

$$\omega_0 = \omega_s + \omega_l \quad \text{for the conservation of energy}$$

and

$\underline{k}_s = -\underline{k}_l = \underline{k}$ for the conservation of momentum (dipole approximation) where ω_s and ω_l are the characteristic frequencies of two plasma modes in a collisionless plasma with the presence of pump field.

Therefore, the induced current density for the S (or L) mode due to the coupling between L (or S) mode and the pump wave can be obtained with the aid of (3.27) and (3.28) as

$$\begin{aligned} \delta \underline{J}_s^-(\underline{k}, t) = & -\sum_{\alpha} \frac{\ln e^3}{\alpha^2} \frac{\omega_o}{\omega_o^2 - \Omega_{\alpha}^2} \left\{ \underline{A}_{\alpha} \cdot (\underline{E}_1^- + \underline{E}_2^-) \int d\underline{v} \int_0^{\infty} d\tau \left\{ \frac{\partial f}{\partial \underline{v}_{\perp}} [\cos(\Omega_{\alpha} \tau + \theta) \hat{x} \right. \right. \\ & + \sin(\Omega_{\alpha} \tau + \theta) \hat{y}] + \frac{\partial f}{\partial \underline{v}_{\parallel}} \hat{z} \} e^{-i\omega_l \tau} e^{-i\phi_{\alpha}(\tau)} \\ & + \left[\frac{\underline{k} \cdot \underline{A}_{\alpha} \cdot (\underline{E}_1^- + \underline{E}_2^-)}{\omega_o} \int d\underline{v} \int_0^{\infty} d\tau \left\{ \frac{\partial f}{\partial \underline{v}_{\perp}} [\cos(\Omega_{\alpha} \tau + \theta) \hat{x} + \sin(\Omega_{\alpha} \tau + \theta) \hat{y}] + \frac{\partial f}{\partial \underline{v}_{\parallel}} \hat{z} \right\} \right. \\ & \left. \left. e^{-i\omega_l \tau} e^{i\phi_{\alpha}(\tau)} (1 - e^{i\omega_o \tau}) \right\} \cdot \delta \underline{E}_l^+(\underline{k}, t) \right. \end{aligned} \quad (3.29)$$

and

$$\begin{aligned} \delta \underline{J}_l^+(\underline{k}, t) = & \sum_{\alpha} \frac{\ln e^3}{\alpha^2} \frac{\omega_o}{\omega_o^2 - \Omega_{\alpha}^2} \left\{ \underline{A}_{\alpha}^* \cdot (\underline{E}_1^+ + \underline{E}_2^+) \int d\underline{v} \int_0^{\infty} d\tau \left\{ \frac{\partial f}{\partial \underline{v}_{\perp}} [\cos(\Omega_{\alpha} \tau + \theta) \hat{x} \right. \right. \\ & + \sin(\Omega_{\alpha} \tau + \theta) \hat{y}] + \frac{\partial f}{\partial \underline{v}_{\parallel}} \hat{z} \} e^{i\omega_s \tau} e^{-i\phi_{\alpha}(\tau)} \\ & - \left[\frac{\underline{k} \cdot \underline{A}_{\alpha}^* \cdot (\underline{E}_1^+ + \underline{E}_2^+)}{\omega_o} \int d\underline{v} \int_0^{\infty} d\tau \left\{ \frac{\partial f}{\partial \underline{v}_{\perp}} [\cos(\Omega_{\alpha} \tau + \theta) \hat{x} + \sin(\Omega_{\alpha} \tau + \theta) \hat{y}] + \frac{\partial f}{\partial \underline{v}_{\parallel}} \hat{z} \right\} \right. \\ & \left. \left. e^{i\omega_s \tau} e^{-i\phi_{\alpha}(\tau)} (1 - e^{-i\omega_o \tau}) \right\} \cdot \delta \underline{E}_s^-(\underline{k}, t) \right. \end{aligned} \quad (3.30)$$

In carrying out those integrations, we specifically choose the wave vector \underline{k} on the x-z plane and write

$$\underline{k} = k_{\perp} \hat{x} + k_{\parallel} \hat{z} \quad (3.31)$$

Equation (3.18) becomes

$$\phi_{\alpha}(\tau) = \mathcal{J}_{\alpha} [\sin(\Omega_{\alpha} \tau + \theta) - \sin \theta] k_{||} v_{||} \tau \quad (3.32)$$

where

$$\mathcal{J}_{\alpha} = k_{\perp} v_{\perp} / \Omega_{\alpha} \quad (3.33)$$

then we have

$$\exp[-i\phi_{\alpha}(\tau)] = \sum_{n=-\infty}^{+\infty} \sum_{n'=-\infty}^{+\infty} J_n(\mathcal{J}_{\alpha}) J_{n'}(\mathcal{J}_{\alpha}) \exp\{-i[n(\Omega_{\alpha} \tau + \theta) - n'\theta + k_{||} v_{||} \tau]\} \quad (3.34)$$

Therefore, we obtain following relation

$$\begin{aligned} \int \underline{v} d\underline{v} \int_0^{\infty} d\tau \left\{ \frac{\partial f_0}{\partial v_{\perp}} [\cos(\Omega\tau + \theta) \hat{x} + \sin(\Omega\tau + \theta) \hat{y}] + \frac{\partial f_0}{\partial v_{||}} \hat{z} \right\} e^{-i\phi(\tau)} e^{i\omega\tau} \\ = \frac{1}{i\omega} \left\{ \sum_{n=-\infty}^{+\infty} \frac{Z_0}{Z_n} \Pi_n^*(\beta, Z_n; n) [1 - W(Z_n)] - Z_0^2 \hat{z} \hat{z} \right\} \end{aligned} \quad (3.35)$$

for a Maxwellian distribution function f_0 .

where

$$Z_n = \frac{\omega - n\Omega}{k_{||}(T/m)^{1/2}}, \quad \beta = k_{\perp}^2 T / m\Omega^2 \quad \text{and} \quad \Lambda_n(\beta) = I_n(\beta) e^{-\beta} \quad (3.36)$$

and

$$\begin{aligned} \Pi(\beta, Z_n; n) = \frac{n^2}{\beta} \Lambda_n(\beta) \hat{x} \hat{x} + \left[\frac{n^2}{\beta} \Lambda_n(\beta) - 2\beta \Lambda_n'(\beta) \right] \hat{y} \hat{y} + Z_n^2 \Lambda_n(\beta) \hat{z} \hat{z} - i n \Lambda_n'(\beta) (\hat{x} \hat{y} - \hat{y} \hat{x}) \\ + \frac{k_{\perp} \Omega}{|k_{\perp} \Omega|} \frac{n}{\sqrt{\beta}} Z_n \Lambda_n(\beta) (\hat{x} \hat{z} + \hat{z} \hat{x}) + \frac{i k_{\perp} \Omega}{|k_{\perp} \Omega|} \sqrt{\beta} Z_n \Lambda_n'(\beta) (\hat{y} \hat{z} - \hat{z} \hat{y}) \end{aligned} \quad (3.37)$$

Substituting (3.35) in (3.29) and (3.30), the results are

$$\begin{aligned}
 \delta \underline{J}_s^-(\underline{k}, t) = & \sum_{\alpha} \frac{n_{\alpha} e^3 \omega_{\alpha 0}}{m_{\alpha} T_{\alpha} (\omega_{\alpha 0}^2 - \Omega_{\alpha}^2)} \delta \underline{E}_l^+(\underline{k}, t) \cdot \left\{ \left[\sum_n \frac{\Omega_{\alpha}}{k_{\perp} (\omega_l + n \Omega_{\alpha})} [1 - W(Z_{ln}^{\alpha})] [n \Lambda_n(\beta_{\alpha}) \hat{x} \right. \right. \\
 & + i \beta_{\alpha} \Lambda_n'(\beta_{\alpha}) \hat{y}] + \frac{W(Z_{ln}^{\alpha})}{k_{\parallel}} \Lambda_n(\beta_{\alpha}) \hat{z} \left. \right] \underline{A}_{\alpha} \\
 & + \frac{\beta_{\alpha} \Omega_{\alpha}^2}{k_{\perp} \omega_{\alpha 0}} \left[\sum_n \frac{1}{k_{\perp} (\omega_l + n \Omega_{\alpha})} \Pi(\beta_{\alpha}, Z_{ln}^{\alpha}; n) [1 - W(Z_{ln}^{\alpha})] - \frac{Z_{l0}^{\alpha 2}}{k_{\perp} \omega_l} \hat{z} \hat{z} \right] [\underline{k} \cdot \underline{A}_{\alpha}] \\
 & + \frac{\beta_{\alpha} \Omega_{\alpha}^2}{k_{\perp} \omega_{\alpha 0}} \left[\sum_n \frac{1}{k_{\perp} (\omega_s - n \Omega_{\alpha})} \Pi(\beta_{\alpha}, Z_{sn}^{\alpha}; n) [1 - W(Z_{sn}^{\alpha})] - \frac{Z_{s0}^{\alpha 2}}{k_{\perp} \omega_s} \hat{z} \hat{z} \right] [\underline{k} \cdot \underline{A}_{\alpha}] \left\{ \right. \\
 & \cdot (\underline{E}_1^- + \underline{E}_2^-)
 \end{aligned} \tag{3.38}$$

and

$$\begin{aligned}
 \delta \underline{J}_l^+(\underline{k}, t) = & \sum_{\alpha} \frac{n_{\alpha} e^3 \omega_{\alpha 0}}{m_{\alpha} T_{\alpha} (\omega_{\alpha 0}^2 - \Omega_{\alpha}^2)} \delta \underline{E}_s^-(\underline{k}, t) \cdot \left\{ \left[\sum_n \frac{\Omega_{\alpha}}{k_{\perp} (\omega_s - n \Omega_{\alpha})} [1 - W(Z_{sn}^{\alpha})] [n \Lambda_n(\beta_{\alpha}) \hat{x} \right. \right. \\
 & + i \beta_{\alpha} \Lambda_n'(\beta_{\alpha}) \hat{y}] - \frac{W(Z_{sn}^{\alpha})}{k_{\parallel}} \Lambda_n(\beta_{\alpha}) \hat{z} \left. \right] \underline{A}_{\alpha}^* \\
 & - \frac{\beta_{\alpha} \Omega_{\alpha}^2}{k_{\perp} \omega_{\alpha 0}} \left[\sum_n \frac{1}{k_{\perp} (\omega_s - n \Omega_{\alpha})} \Pi(\beta_{\alpha}, Z_{sn}^{\alpha}; n) [1 - W(Z_{sn}^{\alpha})] - \frac{Z_{s0}^{\alpha 2}}{k_{\perp} \omega_s} \hat{z} \hat{z} \right] [\underline{k} \cdot \underline{A}_{\alpha}^*] \\
 & - \frac{\beta_{\alpha} \Omega_{\alpha}^2}{k_{\perp} \omega_{\alpha 0}} \left[\sum_n \frac{1}{k_{\perp} (\omega_l + n \Omega_{\alpha})} \Pi(\beta_{\alpha}, Z_{ln}^{\alpha}; n) [1 - W(Z_{ln}^{\alpha})] \right. \\
 & \left. - \frac{Z_{l0}^{\alpha 2}}{k_{\perp} \omega_l} \hat{z} \hat{z} \right] [\underline{k} \cdot \underline{A}_{\alpha}^*] \left\{ \right. \cdot (\underline{E}_1^+ + \underline{E}_2^+)
 \end{aligned} \tag{3.39}$$

where

$$Z_{ln}^{\alpha} = - \frac{\omega_l + n\Omega_{\alpha}}{k_{||}(T_{\alpha}/m_{\alpha})^{\frac{1}{2}}}, \quad Z_{sn}^{\alpha} = \frac{\omega_s - n\Omega_{\alpha}}{k_{||}(T_{\alpha}/m_{\alpha})^{\frac{1}{2}}}, \quad \beta_{\alpha} = k_{\perp}^2 T_{\alpha} / m_{\alpha} \Omega_{\alpha}^2 \quad (3.40)$$

whence the induced polarizations are obtained as

$$\delta \underline{P}_s^{-}(\underline{k}, t) = \frac{i}{\omega_s} \delta \underline{J}_s^{-}(\underline{k}, t) = \delta \underline{E}_l^{+}(\underline{k}, t) \cdot \left(\frac{\partial \underline{\alpha}}{\partial \delta \underline{E}_l^{+}} \right) \cdot \underline{E}^{-} \quad (3.41)$$

$$\delta \underline{P}_l^{+}(\underline{k}, t) = - \frac{i}{\omega_l} \delta \underline{J}_l^{+}(\underline{k}, t) = \delta \underline{E}_s^{-}(\underline{k}, t) \cdot \left(\frac{\partial \underline{\alpha}}{\partial \delta \underline{E}_s^{-}} \right) \cdot \underline{E}^{+} \quad (3.42)$$

where

$$\underline{E}^{-} = \underline{E}_1^{-} + \underline{E}_2^{-} \quad \text{and} \quad \underline{E}^{+} = \underline{E}_1^{+} + \underline{E}_2^{+}$$

IV. DETAILED ANALYSIS OF THRESHOLD POWER AND INITIAL GROWTH RATE

1. Conditions and Properties of the Instabilities Occurring on the Basis of a General Form of the Coupled Mode Equations

In the following paragraph we will show that the coupled wave equations (2.20) and (2.21) derived in Section II can be reduced to the following scalar form similar to those introduced by Nishikawa¹¹:

$$\left[\frac{d^2}{dt^2} + 2\Gamma_s \frac{d}{dt} + \omega_s^2 \right] X = i\lambda Y E^-(t) \quad (4.1)$$

$$\left[\frac{d^2}{dt^2} + 2\Gamma_\ell \frac{d}{dt} + \omega_\ell^2 \right] Y = -i\mu X E^+(t) \quad (4.2)$$

where for simplicity, we treat only the case with

$$\lambda\mu = \text{real} > 0$$

Taking the Fourier transform of (4.1) and (4.2), we obtain

$$\left[\omega^2 - \omega_s^2 + 2i\Gamma_s \omega \right] X(\omega) = \lambda E_0 Y(\omega - \omega_0) \quad (4.3)$$

$$\left[(\omega - \omega_0)^2 - \omega_\ell^2 + 2i\Gamma_\ell (\omega - \omega_0) \right] Y(\omega - \omega_0) = \mu E_0 X(\omega) \quad (4.4)$$

where

$$X(t), Y(t) = \int_{-\infty}^{+\infty} \frac{d\omega}{2\pi} e^{-i\omega t} X(\omega), Y(\omega).$$

Setting the determinant of the coefficient matrix equal to zero, the dispersion relations which determine the frequency and damping (or growing) of the waves under consideration are obtained, namely,

$$\left[\omega^2 - \omega_s^2 + 2i\Gamma_s \omega \right] \left[(\omega - \omega_o)^2 - \omega_\ell^2 + 2i\Gamma_\ell (\omega - \omega_o) \right] - \lambda \mu E_o^2 = 0 \quad (4.5)$$

If the solution of (4.5) is written in the form

$$\omega = x + iy \quad (4.6)$$

then x and $(-y)$ are the frequency and damping rates, respectively, of the new normal mode with parametric coupling effect. It becomes unstable if

$$y > 0 \quad (4.7)$$

Considering first the threshold case in which $y = 0$, $E_o = E_c$ and (4.5) can be separated into two equations

$$\Gamma_s x \left[(x - \omega_o)^2 - \omega_\ell^2 \right] + \Gamma_\ell (x - \omega_o) (x^2 - \omega_s^2) = 0 \quad (4.8)$$

$$(x^2 - \omega_s^2) \left[(x - \omega_o)^2 - \omega_\ell^2 \right] - 4\Gamma_s \Gamma_\ell x (x - \omega_o) - \lambda \mu E_c^2 = 0 \quad (4.9)$$

Since Γ_s and Γ_ℓ are arbitrary, the threshold intensity of the pump field and the frequencies of X and Y are given by

$$x = \omega_s \quad (4.10)$$

$$x - \omega_o = -\omega_\ell \quad (4.11)$$

$$E_c^2 = \frac{4\Gamma_s \Gamma_\ell \omega_s \omega_\ell}{\lambda \mu} \quad (4.12)$$

Thus under the condition of frequency match, there is no frequency shift of X and Y at the threshold.

With the pump field $E_o > E_c$, we no longer can set $y = 0$. Substituting (4.6) in (4.5) and separating the real and imaginary parts, we obtain

$$(x^2 - y^2 - \omega_s^2 - 2\Gamma_s y) \left[(x - \omega_o)^2 - \omega_\ell^2 - 2\Gamma_\ell y \right] - 4x(x - \omega_o)(y + \Gamma_s)(y + \Gamma_\ell) - \lambda \mu E_o^2 = 0 \quad (4.13)$$

$$x(y + \Gamma_s) \left[(x - \omega_o)^2 - y^2 - \omega_\ell^2 - \Gamma_\ell y \right] + (x - \omega_o)(y + \Gamma_\ell)(x^2 - y^2 - \omega_s^2 - 2\Gamma_s y) = 0 \quad (4.14)$$

If the frequency shift is small compared with ω_s , then (4.14) can be approximated as

$$x^2 - y^2 - \omega_s^2 - 2\Gamma_s y = \frac{-2 \left[\omega_\ell (x - \omega_s) + \Gamma_\ell y \right] \omega_s (y + \Gamma_s)}{\omega_\ell \Gamma_\ell} \approx 0 \quad (4.15)$$

and (4.13) becomes

$$4(y + \Gamma_s)(y + \Gamma_\ell) \omega_s \omega_\ell \approx \lambda \mu E_o^2 \quad (4.16)$$

After some algebraic manipulation, we find

$$y = \frac{-(\Gamma_s + \Gamma_\ell) + \sqrt{(\Gamma_\ell - \Gamma_s)^2 + \lambda \mu E_o^2 / \omega_s \omega_\ell}}{2} = \frac{-(\Gamma_s + \Gamma_\ell) + \sqrt{(\Gamma_\ell - \Gamma_s)^2 + 4\Gamma_s \Gamma_\ell E_o^2 / E_c^2}}{2} \quad (4.17)$$

$$x \approx \omega_s + \frac{y(y + 2\Gamma_s)}{2\omega_s} \quad (4.18)$$

In general Γ_ℓ is much larger than Γ_s , therefore we may express (4.17) and (4.18) in the vicinity of the threshold as

$$y \approx \Gamma_s \left[\frac{E_o^2}{E_c^2} - 1 \right] \quad (4.19)$$

$$x \approx \omega_s + \frac{\Gamma_s^2}{2\omega_s} \left[\left(\frac{E_o^2}{E_c^2} \right)^2 - 1 \right] \approx \omega_s + \frac{\Gamma_s^2}{\omega_s} \left[\frac{E_o^2}{E_c^2} - 1 \right] \quad (4.20)$$

The initial exponential growth rate and the frequency shift are linearly proportional to the pump intensity. These results are, however, valid only when the frequency shift is small compared to ω_s and the pump intensity is near the threshold. These phenomena had actually been observed in Stenzel and Wong's²⁰ experiment in an unmagnetized plasma.

2. Parametric Decay into Longitudinal Modes (electrostatic approximation)

Thus we can write

$$\delta \underline{E}_s^-(\underline{k}, t) = -ik\phi_s^-(\underline{k}, t) \quad \text{and} \quad \delta \underline{E}_\ell^+(\underline{k}, t) = -ik\phi_\ell^+(\underline{k}, t) \quad (4.21)$$

and substitute these relations in (2.20) and (2.21). We have

$$\begin{aligned} \left[\frac{d^2}{dt^2} + 2\Gamma_s \frac{d}{dt} + \omega_s^2(\underline{k}) \right] \phi_s^-(\underline{k}, t) &= \frac{M\omega_s^4(\underline{k})}{n_o e^2 k^2} \underline{k} \cdot \left[\frac{\partial(\underline{k} \cdot \underline{\alpha})}{\partial \delta \underline{E}_\ell^+} \right] \cdot \underline{E}^- \phi_\ell^+(\underline{k}, t) \\ &+ \frac{M\omega_s'^2(\underline{k})\Omega_i^2}{n_o e^2 k^2} \underline{k} \cdot \left\{ \hat{z} \times \left[\underline{k} \cdot \left(\frac{\partial \underline{\alpha}}{\partial \delta \underline{E}_\ell^+} \right) \right] \cdot \underline{E}^- \right\} \phi_\ell^+(\underline{k}, t) \end{aligned} \quad (4.22)$$

$$\begin{aligned} \left[\frac{d^2}{dt^2} + 2\Gamma_\ell \frac{d}{dt} + \omega_\ell^2(\underline{k}) \right] \phi_\ell^+(\underline{k}, t) &= \frac{m\omega_\ell^4(\underline{k})}{n_o e^2 k^2} \underline{k} \cdot \left[\frac{\partial(\underline{k} \cdot \underline{\alpha})}{\partial \delta \underline{E}_s^-} \right] \cdot \underline{E}^+ \phi_s^-(\underline{k}, t) \\ &+ \frac{m\omega_\ell'^2(\underline{k})\Omega_e^2}{n_o e^2 k^2} \underline{k} \cdot \left\{ \hat{z} \times \left[\underline{k} \cdot \left(\frac{\partial \underline{\alpha}}{\partial \delta \underline{E}_s^-} \right) \right] \cdot \underline{E}^+ \right\} \phi_s^-(\underline{k}, t) \end{aligned} \quad (4.23)$$

(a) When the pump wave is the ordinary mode and the decay waves are ion acoustic mode and electron plasma mode

$$\text{Let } \underline{E}(t) = 2E_2 \cos \omega_0 t \hat{z} \quad (\text{i. e., } \underline{E}_1 = 0)$$

and

(4. 24)

$$\underline{k} = k \hat{z} \quad (\text{i. e., } k_{\parallel} = k, k_{\perp} = 0, \beta_{\alpha} = 0)$$

and the substitution of (4. 24) into (4. 22) and (4. 23) will yield

$$\left[\frac{d^2}{dt^2} + 2\Gamma_s \frac{d}{dt} + \omega_s^2(k) \right] \phi_s^-(k, t) = \frac{iM\omega_s^4}{n_o e^2 k} \sum_{\alpha} \frac{n_{\alpha} e_{\alpha}^3}{\alpha m_{\alpha} T_{\alpha} \omega_o^2} \left\{ W\left(-\frac{\omega_l}{k \sqrt{T_{\alpha}/m_{\alpha}}}\right) - W\left(\frac{\omega_s}{k \sqrt{T_{\alpha}/m_{\alpha}}}\right) \right\} E_2 \phi_{\ell}^+(k, t) \quad (4. 25)$$

$$\left[\frac{d^2}{dt^2} + 2\Gamma_{\ell} \frac{d}{dt} + \omega_{\ell}^2(k) \right] \phi_{\ell}^+(k, t) = \frac{i m \omega_{\ell}^4}{n_o e^2 k} \sum_{\alpha} \frac{n_{\alpha} e_{\alpha}^3}{\alpha m_{\alpha} T_{\alpha} \omega_o^2} \left\{ W\left(\frac{\omega_s}{k \sqrt{T_{\alpha}/m_A}}\right) - W\left(-\frac{\omega_l}{k \sqrt{T_{\alpha}/m_{\alpha}}}\right) \right\} E_2 \phi_s^-(k, t) \quad (4. 26)$$

Since the decay modes we are considering are in the frequency domains such that

$$\sqrt{T_i/M} \ll \omega_s/k \ll \sqrt{T_e/m} \ll \omega_{\ell}/k \quad (4. 27)$$

then (4. 25) and (4. 26) become

$$\left[\frac{d^2}{dt^2} + 2\Gamma_s \frac{d}{dt} + \omega_s^2 \right] \phi_s^-(k, t) = i \frac{k e \omega_s^2}{m \omega_o^2} \phi_{\ell}^+(k, t) E^-(t) \quad (4. 28)$$

$$\left[\frac{d^2}{dt^2} + 2\Gamma_\ell \frac{d}{dt} + \omega_\ell^2 \right] \phi_\ell^+(k, t) = -i \frac{ke}{m} \frac{k_d^2}{k^2} \phi_s^-(k, t) E^+(t) \quad (4.29)$$

where we have used relations

$$\omega_s^2 = k^2 T_e / M, \quad \omega_\ell^2 \approx \omega_{pe}^2 = \frac{4\pi n_o e^2}{m} \approx \omega_o^2 \quad \text{and} \quad k_d^2 = \frac{4\pi n_o e^2}{T_e} \quad (4.30)$$

Equations (4.28) and (4.29) had been obtained by Nishikawa¹¹, who worked with a hydrodynamic model. If we take the Fourier transform of (4.28) and (4.29), the results would be the same as DuBois and Goldman¹⁰, Nishikawa¹¹, Lee and Su¹², and Jackson's¹³ conclusions.

Therefore, the threshold field is given by

$$\frac{E_{th}}{8\sqrt{\pi n_o T_e}} = \sqrt{\frac{\Gamma_s \Gamma_\ell}{\omega_s \omega_\ell}} \quad (4.31)$$

where $E_{th} = 2E_2$.

(b) When the pump field is extraordinary mode ($E \perp B_o$) and $|\Omega_e| \gg \omega_{pe}$.

In this case we may write

$$\underline{E} = 2E_o(\hat{x} \cos \omega_o t - \hat{y} \sin \omega_o t) \quad (\text{i. e., } \underline{E}_2 = \hat{x} E_o, \underline{E}_1 = -\hat{y} E_o)$$

and

$$\underline{k} = k_\perp \hat{x} + k_\parallel \hat{z} \quad (4.32)$$

Substituting (4.32) in (4.22) and (4.23), we obtain

$$\left[\frac{d^2}{dt^2} + 2\Gamma_s \frac{d}{dt} + \omega_s^2 \right] \phi_s^-(k, t) = \frac{iM\omega_s^4}{n_o e^2 k^2} (k_\perp \epsilon P_{s1}^- + k_\parallel \epsilon P_{s3}^-) + \frac{iM\omega_s^2 \Omega_i^2}{n_o e^2 k^2} k_\perp \epsilon P_{s1}^- \quad (4.33)$$

$$\left[\frac{d^2}{dt^2} + 2\Gamma_\ell \frac{d}{dt} + \omega_\ell^2 \right] \phi_\ell^+(\underline{k}, t) = \frac{im\omega_\ell^4}{n_o e^2 k^2} (k_\perp \delta P_{\ell 1}^+ + k_\parallel \delta P_{\ell 3}^+) + \frac{im\omega_\ell^2 \Omega_e^2}{n_o e^2 k^2} k_\perp \delta P_{\ell 1}^+ \quad (4.34)$$

where

$$\delta P_{s1}^- = \frac{1}{\omega_s} \sum_\alpha \frac{n_\alpha e^3 \omega_o (1 + \frac{\Omega_\alpha}{\omega_o})}{m_\alpha T_\alpha (\omega_o^2 - \Omega_\alpha^2)} \sum_n \left\{ \frac{n \Omega_\alpha \Lambda_n(\beta_\alpha)}{(\omega_\ell + n \Omega_\alpha)} \left(1 + \frac{n \Omega_\alpha}{\omega_o} \right) \left[1 - W(Z_{\ell n}^\alpha) \right] + \frac{n^2 \Omega_\alpha^2 \Lambda_n(\beta_\alpha)}{\omega_o (\omega_s - n \Omega_\alpha)} \left[1 - W(Z_{sn}^\alpha) \right] + W(Z_{\ell n}^\alpha) \Lambda_n(\beta_\alpha) + \frac{n \Omega_\alpha \Lambda_n(\beta_\alpha)}{\omega_o} \left[W(Z_{\ell n}^\alpha) - W(Z_{sn}^\alpha) \right] \right\} \phi_\ell^+(\underline{k}, t) E_o e^{-i\omega_o t} \quad (4.35)$$

$$\delta P_{s3}^- = \frac{1}{\omega_s} \sum_n \frac{n_\alpha e^3 \omega_o (1 + \frac{\Omega_\alpha}{\omega_o})}{m_\alpha T_\alpha (\omega_o^2 - \Omega_\alpha^2)} \sum_n - \frac{k_\perp}{k_\parallel} \left\{ \frac{\Lambda_n(\beta_\alpha)}{\omega_o} \left[\omega_\ell W(Z_{\ell n}^\alpha) + \omega_s W(Z_{sn}^\alpha) \right] \right\} \phi_\ell^+(\underline{k}, t) E_o e^{-i\omega_o t} \quad (4.36)$$

$$\delta P_{\ell 1}^+ = - \frac{1}{\omega_\ell} \sum_\alpha \left\{ \frac{n_\alpha e^3 \omega_o (1 + \frac{\Omega_\alpha}{\omega_o})}{m_\alpha T_\alpha (\omega_o^2 - \Omega_\alpha^2)} \sum_n \frac{n \Omega_\alpha \Lambda_n(\beta_\alpha)}{(\omega_s - n \Omega_\alpha)} \left(1 - \frac{n \Omega_\alpha}{\omega_o} \right) \left[1 - W(Z_{sn}^\alpha) \right] - \frac{n^2 \Omega_\alpha^2 \Lambda_n(\beta_\alpha)}{\omega_o (\omega_\ell + n \Omega_\alpha)} \left[1 - W(Z_{\ell n}^\alpha) \right] - W(Z_{sn}^\alpha) \Lambda_n(\beta_\alpha) - \frac{n \Omega_\alpha \Lambda_n(\beta_\alpha)}{\omega_o} \left[W(Z_{\ell n}^\alpha) - W(Z_{sn}^\alpha) \right] \right\} \phi_s^-(\underline{k}, t) E_o e^{i\omega_o t} \quad (4.37)$$

$$\delta P_{l3}^+ = \frac{1}{\omega_l} \sum_{\alpha} \frac{n_{\alpha} e^2 \omega_o (1 + \frac{\Omega_{\alpha}}{\omega_o})}{m_{\alpha} T_{\alpha} (\omega_o^2 - \Omega_{\alpha}^2)} \sum_n - \frac{k_{\perp}}{k_{\parallel}} \left\{ \frac{\Lambda_n(\beta_{\alpha})}{\omega_o} \left[\omega_l W(Z_{ln}^{\alpha}) \right. \right. \\ \left. \left. + \omega_s W(Z_{sn}^{\alpha}) \right] \right\} \phi_s^-(\underline{k}, t) E_o e^{i\omega_o t} \quad (4.38)$$

(i) Decay waves are electrostatic ion cyclotron wave (ion acoustic wave) and upper-hybrid wave

Thus, we may assume $\sqrt{\frac{m}{M}} \ll k_{\parallel}/k_{\perp} \ll 1$ such that $W(Z_{ln}^{\alpha}) \approx 0$, and $W(Z_{sn}^i) \approx 0$ for all n and $W(Z_{sn}^e) \approx 0$ for $n \neq 0$, $W(Z_{s0}^e) \Lambda_o(\beta_o) \approx 1$.

With these approximations, equations (4.35)-(4.38) may be reduced to

$$\delta P_{s1}^- = \frac{n_o e^3}{2\omega_l^2 m T_e} \frac{k_{\perp}^2}{k_d^2}$$

$$\delta P_{s3}^- \approx \frac{n_o e^3}{2\omega_l^2 m T_e} \frac{k_{\perp}}{k_{\parallel}} \quad (4.39)$$

$$\delta P_{l1}^+ \approx - \frac{n_o e^3}{2m T_e \omega_l^2} (1 + k_{\perp}^2/k_d^2)$$

$$\delta P_{l3}^+ \approx 0$$

and (4.33) and (4.34) become

$$\left[\frac{d^2}{dt^2} + 2\Gamma_s \frac{d}{dt} + \omega_s^2 \right] \phi_s^-(\underline{k}, t) = \frac{i M e \omega_s^4}{2 k m T_e \omega_l^2} (1 + k_{\perp}^2/k_d^2) E_o e^{-i\omega_o t} \phi_l^+(\underline{k}, t) \quad (4.40)$$

$$\left[\frac{d^2}{dt^2} + 2\Gamma_l \frac{d}{dt} + \omega_l^2 \right] \phi_l^+(\underline{k}, t) = \frac{-i e \omega_l^2 (1 + k_{\perp}^2/k_d^2)}{k T_e} E_o e^{i\omega_o t} \phi_s^-(\underline{k}, t) \quad (4.41)$$

Therefore, the threshold field can be calculated as

$$\frac{E_{th}}{8\sqrt{\pi n_o T_e}} = \sqrt{\frac{\Gamma_s \Gamma_l}{\omega_s \omega_l}} \frac{\omega_l}{\omega_{pe}} \quad (4.42)$$

where $E_{th} = (2E_o)_{th}$, $\omega_s^2 = \Omega_i^2 + \frac{k_{\perp}^2 T_e / M}{1 + k_{\perp}^2 / k_d^2} \approx \frac{k_{\perp}^2 T_e / M}{1 + k_{\perp}^2 / k_d^2}$ and $k_{\perp}^2 / k_d^2 \approx 1$. This had been obtained by Porkolah²¹.

(ii) Decay waves are lower hybrid and upper hybrid waves

In this case $k_{\parallel} / k_{\perp} \ll \sqrt{\frac{m}{M}}$, therefore $W(Z_n) = 0$ for all n .

Since $\omega_o = \frac{|\Omega_e|}{2} + \sqrt{\left(\frac{\Omega_e}{2}\right)^2 + \omega_{pe}^2} \approx |\Omega_e| + \frac{\omega_{pe}^2}{|\Omega_e|} = \omega_l + \omega_s$, and

$$\beta_e = k_{\perp}^2 T_e / m \Omega_e^2 = \frac{k_{\perp}^2}{k_d^2} \frac{\omega_{pe}^2}{\Omega_e^2} \geq 1, \quad \omega_l \approx |\Omega_e| + \frac{\omega_{pe}^2}{|\Omega_e|} \Lambda_1(\beta_e) \approx |\Omega_e|$$

$$\Rightarrow \omega_{pe}^2 \approx |\Omega_e| \omega_s$$

and $\omega_l \approx |\Omega_e| + \omega_s \Lambda_1(\beta_e)$; $k_{\perp}^2 \approx k_d^2 \frac{|\Omega_e|}{\omega_s}$.

With these approximations, equations (4.35) - (4.38) become

$$\delta P_{s1}^- = \frac{n_o e^3}{m T_e \omega_{pe}^2} \phi_l^+(k, t) E_o e^{-i\omega_o t}$$

$$\delta P_{s3}^- = 0$$

$$\delta P_{l1}^+ = - \frac{n_o e^3}{m T_e \omega_{pe}^2} \phi_s^-(k, t) E_o e^{i\omega_o t}$$

$$\delta P_{l3}^+ = 0$$

and (4.33) and (4.34) become

(4.43)

$$\left[\frac{d^2}{dt^2} + 2\Gamma_s \frac{d}{dt} + \omega_s^2 \right] \phi_s^-(\underline{k}, t) = \frac{iM e \omega_s^4}{k m T_e \omega_{pe}^2} \phi_\ell^+(\underline{k}, t) E_o e^{-i\omega_o t} \quad (4.44)$$

$$\left[\frac{d^2}{dt^2} + 2\Gamma_\ell \frac{d}{dt} + \omega_\ell^2 \right] \phi_\ell^+(\underline{k}, t) = - \frac{2ie \omega_\ell^4}{T_e \omega_{pe}^2 k} \phi_s^-(\underline{k}, t) E_o e^{i\omega_o t} \quad (4.45)$$

Therefore; the threshold field can be calculated as

$$\frac{E_{th}}{8 \sqrt{\pi n_o T_e}} = \sqrt{\frac{\Gamma_s \Gamma_\ell}{\omega_s \omega_\ell}} \frac{\omega_{pe}}{\sqrt{2\omega_s |\Omega_e|}} \quad (4.46)$$

which also agrees with Porkolab's²¹ result.

$$\text{where } E_{th} = (2E_o)_{th}, \quad \omega_s^2 = |\Omega_e \Omega_i| \left[\frac{\omega_{pe}^2 + |\Omega_e \Omega_i|}{\omega_{pe}^2 + \Omega_e^2} \right] \approx \omega_{pi}^2$$

(c) For a forced linearly polarized pump field with upper hybrid and lower hybrid waves as decay waves

In this case we write $\underline{E} = 2E_o \cos \omega_o t \hat{x}$ (i. e. $\underline{E}_2 = \hat{x} E_o$; $\underline{E}_1 = 0$)

and $\underline{k} = k_\perp \hat{x} + k_\parallel \hat{z}$ ($k_\parallel / k_\perp \ll \sqrt{\frac{m}{M}}$)

Since $\omega_o^2 \approx \Omega_e^2 + \omega_{pe}^2$, $\beta_e = k_\perp^2 T_e / m \Omega_e^2 \approx \omega_{pe}^2 / \Omega_e^2 \ll 1$ and $\omega_s \approx \omega_{pi}$.

With these approximations; equations (4.33) and (4.34) become

$$\left[\frac{d^2}{dt^2} + 2\Gamma_s \frac{d}{dt} + \omega_s^2 \right] \phi_s^-(\underline{k}, t) = \frac{iM e \omega_s^4}{m T_e k \omega_{pe}^2} \phi_\ell^+(\underline{k}, t) E_o e^{-i\omega_o t} \quad (4.47)$$

$$\left[\frac{d^2}{dt^2} + 2\Gamma_\ell \frac{d}{dt} + \omega_\ell^2 \right] \phi_\ell^+(\underline{k}, t) = \frac{-2ie \omega_\ell^4}{\omega_{pe}^2 T_e k} \phi_s^-(\underline{k}, t) E_o e^{i\omega_o t} \quad (4.48)$$

Therefore, the threshold field is given as

$$\frac{E_{th}}{8\sqrt{\pi n_o T_e}} = \sqrt{\frac{\Gamma_l \Gamma_s}{\omega_s \omega_l}} \frac{\omega_{pe}}{\sqrt{2} \omega_l} \quad (4.49)$$

3. Parametric Decay into Electrostatic Ion Cyclotron Wave and Harmonics of Electron Cyclotron Wave (Hybrid Mode) in a Uniform Magneto Plasma

For the harmonics of electron cyclotron modes, $|\underline{k}|$ is small ($|\underline{k}| \ll k_d$) such that $\beta_e \ll 1$, and $W(Z_{ln}^e) \approx 0$ for all n .

Since the electrostatic ion cyclotron mode is longitudinal wave, we may assume $\delta \underline{E}_s^-(\underline{k}, t) = -ik \phi_s^-(\underline{k}, t)$, where $\underline{k} = k_{\perp} \hat{x} + k_{\parallel} \hat{z}$ with $\sqrt{\frac{m}{M}} \ll |k_{\parallel}/k_{\perp}| \ll 1$. Therefore, $W(Z_{sn}^e) \approx 0$ for $n \neq 0$ and $W(Z_{s0}^e) \Lambda_o(\beta_e) \approx 1$.

Because the nonlinear coupling due to electrons of the plasma is much stronger than due to ions; therefore we may neglect the ion terms of equations (3.41) and (3.42). The resulting components of the induced polarizations can be simplified to

$$\begin{aligned} \underline{k} \cdot \delta \underline{P}_s^-(\underline{k}, t) = & -\frac{i}{\omega} \frac{n_o e^3 \omega_o}{m T_e (\omega_o^2 - \Omega_e^2)} \delta \underline{E}_l^+ \cdot \left\{ -\frac{\beta_e \omega_l^2 \omega_s}{k_{\perp} \omega_o (\omega_l^2 - \Omega_e^2)} \hat{x} \right. \\ & \left. + \frac{i \beta_e \Omega_e^3 \omega_s}{k_{\perp} \omega_o \omega_l (\omega_l^2 - \Omega_e^2)} \hat{y} - \frac{\omega_s}{k_{\parallel} \omega_o} \hat{z} \right\} \left[\underline{k} \cdot \underline{A}_e \cdot \underline{E}^- \right] \end{aligned} \quad (4.50)$$

$$\begin{aligned} k_{\perp} \delta P_{s1}^-(\underline{k}, t) = & -\frac{i}{\omega_s} \frac{n_o e^3 \omega_o}{m T_e (\omega_o^2 - \Omega_e^2)} \delta \underline{E}_l^+ \cdot \left\{ \frac{-\beta_e \omega_s \omega_l^2}{k_{\perp} \omega_o (\omega_l^2 - \Omega_e^2)} \hat{x} \right. \\ & \left. + \left[\frac{-i \omega_s \beta_e (\omega_l^2 - \Omega_e^2 - \omega_l \Omega_e)}{k_{\perp} \omega_o (\omega_l^2 - \Omega_e^2)} - \frac{i \beta_e \Omega_e}{k_{\perp} \omega_o} \right] \hat{y} \right\} \left[k_{\perp} \hat{x} \cdot \underline{A}_e \cdot \underline{E}^- \right] \end{aligned} \quad (4.51)$$

$$\delta P_{\ell 1}^+(\underline{k}, t) = \frac{1}{\omega_{\ell}} \frac{n_o e^3 \omega_o}{m T_e (\omega_o^2 - \Omega_e^2)} \phi_s^-(\underline{k}, t) \underline{k} \cdot \left\{ \frac{-\beta_e \omega_{\ell}^3}{k_{\perp} \omega_o (\omega_{\ell}^2 - \Omega_e^2)} \hat{x} \right. \\ \left. + \frac{i \beta_e \Omega_e \omega_{\ell}^2}{k_{\perp} \omega_o (\omega_{\ell}^2 - \Omega_e^2)} \hat{y} - \frac{1}{k_{\parallel}} \hat{z} \right\} \left[\hat{x} \cdot \underline{A}_e^* \cdot \underline{E}^+ \right] \quad (4.52)$$

$$\delta P_{\ell 2}^+(\underline{k}, t) = \frac{1}{\omega_{\ell}} \frac{n_o e^3 \omega_o}{m T_e (\omega_o^2 - \Omega_e^2)} \phi_s^-(\underline{k}, t) \underline{k} \cdot \left\{ \frac{-i \beta_e \Omega_e \omega_{\ell}^2}{k_{\perp} \omega_o (\omega_{\ell}^2 - \Omega_e^2)} \hat{x} \right. \\ \left. - \frac{\beta_e \Omega_e^2 \omega_{\ell}}{k_{\perp} \omega_o (\omega_{\ell}^2 - \Omega_e^2)} \hat{y} - i \frac{\Omega_e}{k_{\parallel} \omega_o} \hat{z} \right\} \left[\hat{x} \cdot \underline{A}_e^* \cdot \underline{E}^+ \right] \quad (4.53)$$

$$\delta P_{\ell 3}^+(\underline{k}, t) = \frac{-1}{\omega_{\ell}} \frac{n_o e^3 \omega_o}{m T_e (\omega_o^2 - \Omega_e^2)} \phi_s^-(\underline{k}, t) \left[\hat{z} \cdot \underline{A}_e^* \cdot \underline{E}^+ \right] \quad (4.54)$$

and the coupled mode equations are given by equations (4.33) and (2.21). From (4.52), (4.53) and (2.21), we obtain the relation $\delta E_{\ell 2}^+(\underline{k}, t) = i \frac{\Omega_e}{\omega_o} \delta E_{\ell 1}^+(\underline{k}, t)$, thus the dispersion relation for the L mode is given as

$$1 - \frac{k_d^2}{k^2} \sum_n \frac{(n \Omega_e)^2 \Lambda_n(\beta_e)}{\omega_{\ell} (\omega_{\ell} - n \Omega_e)} = \frac{\Omega_e}{\omega_o} \frac{\omega_{pe}^2}{\omega_{\ell}^2} \sum_n \frac{\omega_{\ell}}{\omega_{\ell} - n \Omega_e} n \Lambda_n'(\beta_e) \quad (4.55)$$

let $\omega_{\ell} = |n \Omega_e| (1 + \Delta_n)$ where $n \geq 2$ and substitute into (4.55), we have

$$\Delta_n = \frac{k_d^2 (n+1) \Lambda_n}{k^2 n (1 - \frac{(n^2+1) \omega_{pe}^2}{n^2 (n^2-1) \Omega_e^2})} \quad (4.56)$$

Since the polarization of the harmonics of electron cyclotron wave can be determined from linear dielectric tensor as

$$\frac{\delta E_{\ell 3}^+}{\delta E_{\ell 1}^+} = \frac{k_{\parallel}}{k_{\perp}} \frac{1}{1 - \left(\frac{\omega_{\ell}}{kc}\right)^2 \left(1 - \frac{\omega_{pe}^2}{\omega_{\ell}^2}\right)} \quad (4.57)$$

thus the linearly polarized pump field can be written as

$$\underline{E} = \left[\hat{x} + \hat{z} \frac{k_{\parallel}}{k_{\perp}} \frac{\omega_o^2 + \Omega_e^2}{\omega_o^2 - \Omega_e^2} \frac{1}{1 - \left(\frac{\omega_{\ell}}{kc}\right)^2 \left(1 - \frac{\omega_{pe}^2}{\omega_{\ell}^2}\right)} \right] 2E_o \cos \omega_o t$$

Therefore, the resulting coupled mode equations are given as

$$\left[\frac{d^2}{dt^2} + 2\Gamma_s \frac{d}{dt} + \omega_s^2 \right] \phi_s^-(\underline{k}, t) = - \frac{M\omega_s^4 e}{k^2 m T_e (\omega_o^2 - \Omega_e^2)} \left[\frac{1}{1 - \left(\frac{\omega_{\ell}}{kc}\right)^2 \left(1 - \frac{\omega_{pe}^2}{\omega_{\ell}^2}\right)} - \frac{|\Omega_i \Omega_e|}{\omega_s \omega_o} \right] \delta E_{\ell 1}^+(\underline{k}, t) E_o e^{-i\omega_o t} \quad (4.58)$$

$$\left[\frac{d^2}{dt^2} + 2\Gamma_{\ell} \frac{d}{dt} + \omega_{\ell}^2 \right] \delta E_{\ell 1}^+(\underline{k}, t) = - \frac{\omega_{\ell}^2 (\omega_{\ell}^2 + \Omega_e^2) e}{T_e (\omega_o^2 - \Omega_e^2)} \phi_s^- E_o e^{i\omega_o t} \quad (4.59)$$

and the threshold field can be calculated as

$$\frac{E_{th}}{8\sqrt{\pi n_o T_e}} = \left(\frac{\Gamma_s \Gamma_{\ell}}{\omega_s \omega_{\ell}} \right)^{1/2} \frac{\omega_o^2 - \Omega_e^2}{(\omega_{\ell}^2 + \Omega_e^2)^{1/2} \omega_{pe}} \left[\frac{1}{1 - \left(\frac{\omega_{\ell}}{kc}\right)^2 \left(1 - \frac{\omega_{pe}^2}{\omega_{\ell}^2}\right)} - \frac{|\Omega_i \Omega_e|}{\omega_s \omega_o} \right]^{-1/2} \quad (4.60)$$

4. Comparison Between Theory and Experiments

a. In the case of parametric decay into electrostatic ion cyclotron wave and second harmonics of electron cyclotron wave in a uniform magneto plasma. (My experiment)

With the aid of (4.60), the value of parameters can be found from Table 2, the threshold field E_{th} is calculated as

$$E_{th} = 13.7 \text{ volts/cm}$$

Near the microwave horn, the pump field is almost uniformly distributed on the cross-section of the chamber, hence the theoretically predicted threshold pump power may be calculated as

$$\text{Threshold pump power} \approx \frac{E_{th}^2}{8\pi} \times \pi r^2 \times c \approx 44 \text{ watts}$$

where $r = 7.5 \text{ cm}$ is the radius of the chamber.

The threshold pump power, experimentally determined, is about 47.1 watts as shown in Figure 10. This value is very close to the theoretically predicted value, and the extra 3 watts is believed to be used to sustain the plasma.

b. In the case of parametric decay into lower hybrid wave at upper hybrid resonance with a linearly polarized pump. (S. Hiroe and H. Ikegami's²² experiment.)

$$T_e = 4 \text{ eV} \quad T_i = 300^\circ \text{K} \quad N = 3.4 \text{ m torr}$$

$$\omega_s = 2\pi \times 3.5 \times 10^4 \text{ sec}^{-1} \quad \omega_l = 2\pi \times 4.1 \times 10^9 \text{ sec}^{-1} = \omega_o$$

$$B_o = 1350 \text{ Gauss} \quad \Omega_i = 2\pi \times 1.05 \times 10^4 \text{ sec}^{-1} \quad \Omega_e = 2\pi \times 3.85 \times 10^9 \text{ sec}^{-1}$$

$$\omega_{pe} = 2\pi \times 1.4 \times 10^9 \text{ sec}^{-1}, \quad \omega_{pi} = 2\pi \times 2.48 \times 10^6 \text{ sec}^{-1}, \quad n_o = 2.42 \times 10^{10} \text{ cm}^{-3}$$

$$\Gamma_\ell = \frac{\nu_{en}}{2} = 3.5 \times 10^7 \text{ sec}^{-1} \quad \Gamma_s = \frac{\nu_{in}}{2} = \frac{1}{2} \sqrt{\frac{m_e}{m_i} \frac{T_i}{T_e}} \nu_{en} = 0.5 \times 10^4 \text{ sec}^{-1}$$

$$m_e = 0.91 \times 10^{-27} \text{ g} \quad m_i = 200 \times 1.67 \times 10^{-24} \text{ g}$$

From (4.49), the electric field associated with the threshold power can be calculated and the result is

$$E_{th} = 2.25 \text{ V/cm}$$

and the experimentally measured threshold field is about 2 V/cm.

V. DESCRIPTION OF EXPERIMENT AND RESULTS

Although the theories⁹⁻¹³ and experiments^{20, 23, 24} of parametric coupling between longitudinal electron plasma waves and ion acoustic waves in an unmagnetized plasma have been treated extensively by various authors, only recently did experiments^{2, 5, 7, 22} in magnetized plasma report on the decay instability. Porkolab and his colleagues have done a series of experimental studies of plasma heating due to the parametric decay instability of plasma waves in a magnetic field and a high-frequency electric field. These decay waves have relatively short wavelengths and broad spectra such that quasi-electrostatic modes may be assumed and an anomalous heating process can be achieved. In our experiment, we have a relatively small sized plasma beam. Working on the slab model, the excited waves are of standing wave type with well defined boundary conditions. Therefore, the frequency spectra of the unstable waves are sharply spiked. The object of the present work is to study both experimentally and theoretically the threshold and saturation of the parametric decay instability of the second harmonic of the electron cyclotron wave and ion acoustic wave.

1. Experimental Apparatus and Procedure

The experiment is performed in a hollow-cathode-arc-discharge (HCD) plasma source²⁵, 15 cm in diameter and a vacuum chamber 2m in length, as shown in Figure 1. The 2m long stainless steel vacuum chamber is separated into two sections, a source region and a drift region, by a baffle. In order to get a highly ionized and confined argon plasma beam in the drift region, the magnetic field in the source region is a mirror field, hence it is hard to get a totally quiescent plasma. In

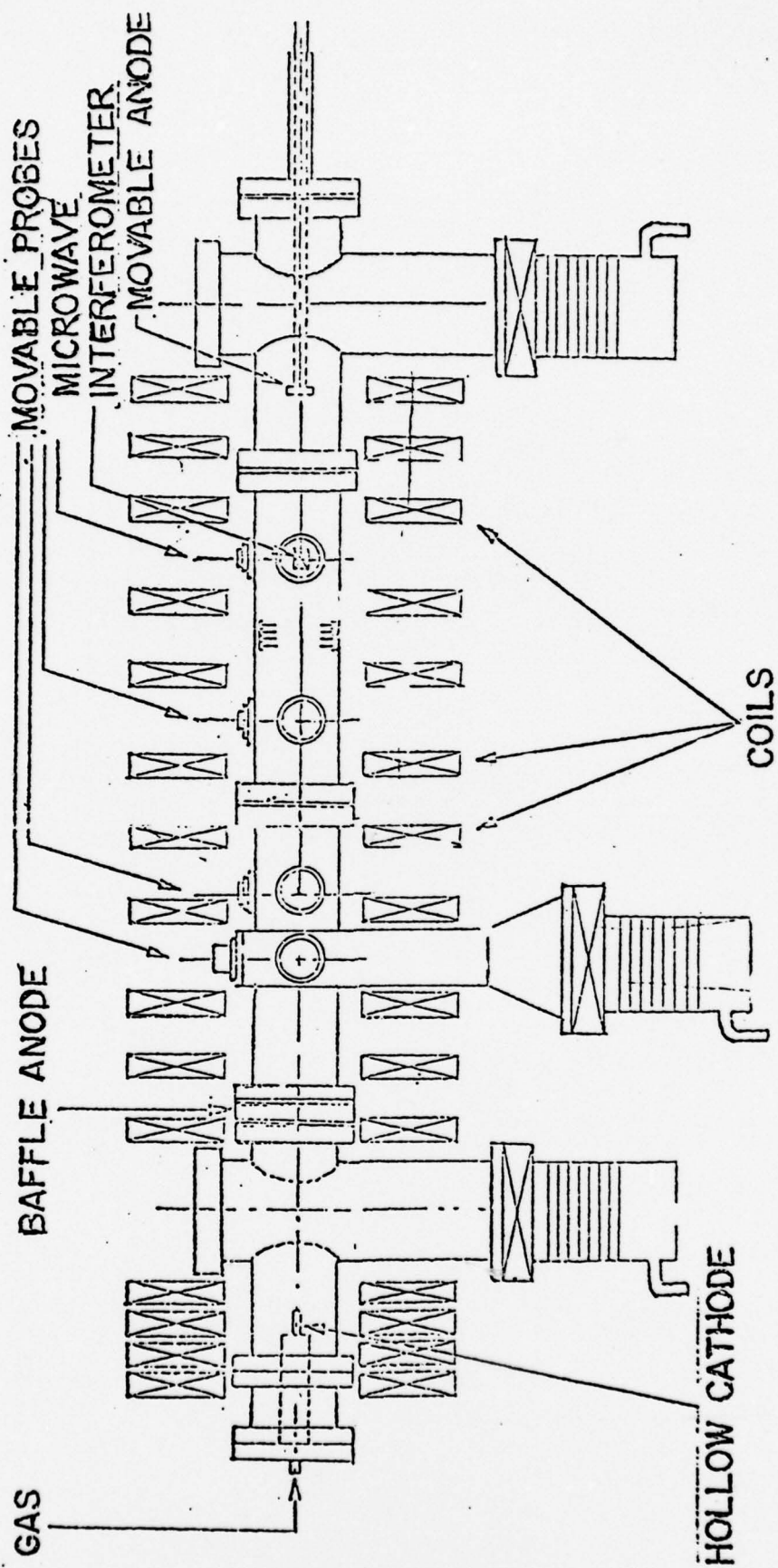


FIGURE 1: SCHEMATIC DIAGRAM OF PINY HCD SYSTEM

our experiment a new procedure is introduced to create an ultrastable microwave sustained plasma. An antenna horn is mounted on the anode and to send the high power microwave (150-200 watts) into the HCD plasma beam. Increasing the drift magnetic field and background gas pressure to a suitably high range (1.5 KG-2KG, $1\ \mu$ - 1.5μ of mercury pressure), we can then shut off the source plasma completely by setting the cathode gas flow and baffle current to zero. Yet the plasma still exists in the drift region sustained by the input microwave. This plasma is very quiescent and well confined in a beam. Adjusting the experimental parameters (such as drift magnetic field, drift gas pressure, microwave power, etc.) to proper values to achieve optimum operating conditions, we obtain a spectrum as in Figure 3, showing the instability and its harmonics due to parametric excitation.

A simplified block diagram of the experimental apparatus is shown in Figure 2. A frequency stabilized Klystron unit, operated in x-band is used as the microwave source. For the measurements of the growth and decay times of the excited waves, a fast PIN diode switch having 20 nanosecond rise and fall times is used to modulate the microwave signal which is fed into a Klystron amplifier, capable of 1K watts cw output at the frequency of 9.23 GHz. Between the PIN diode and the source two variable attenuators are used to adjust the output levels.

Microwave power is transmitted through waveguide into the plasma by means of a horn. Since the EM wave in the waveguide is TE_{10} mode, the electric field in the chamber is linearly polarized in the direction perpendicular to the uniform magnetic field and almost uniformly distributed at the cross-section of the chamber near the horn. The diagnostic devices employed in this experiment include axially and radially movable Langmuir probes.

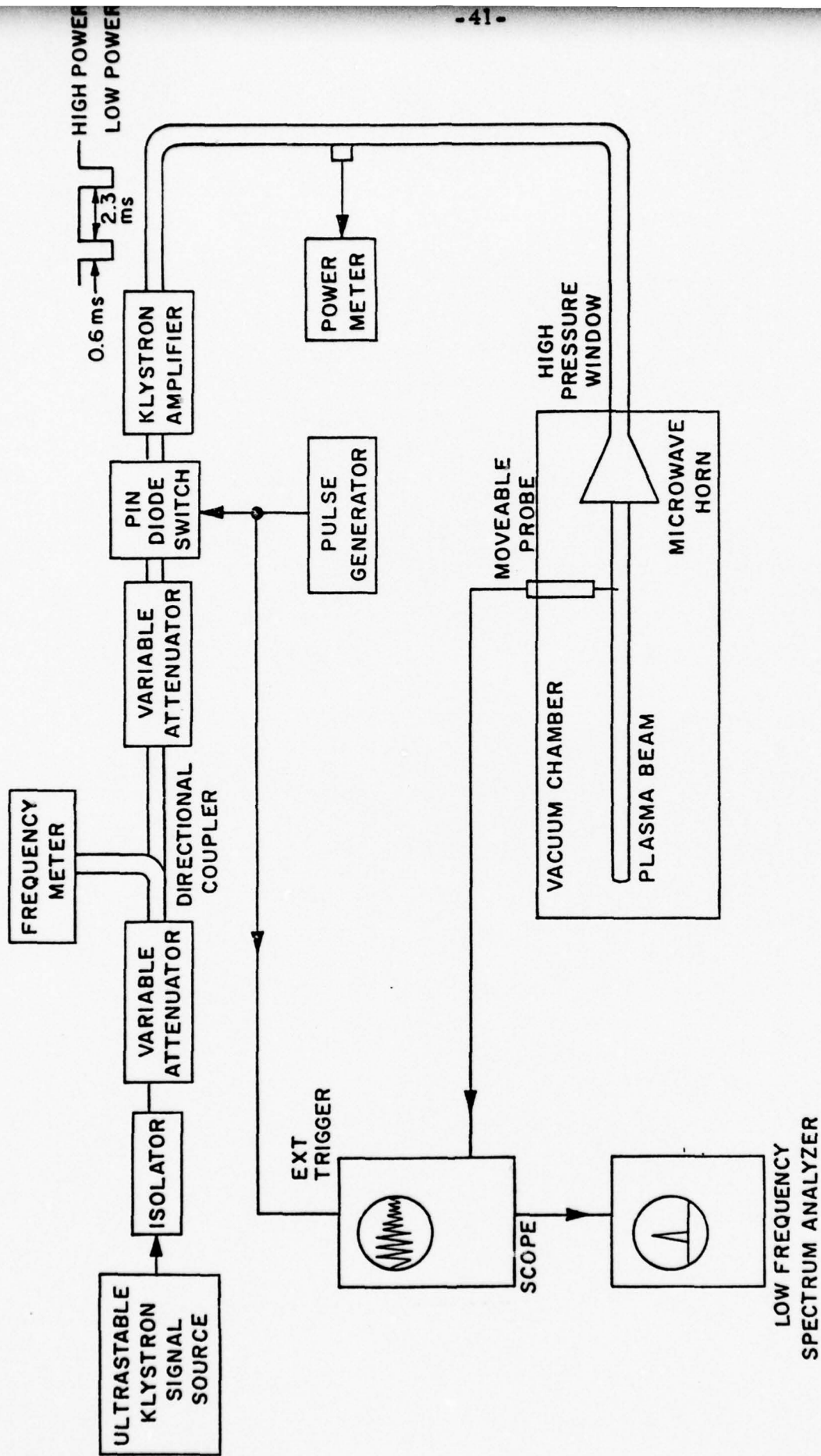


FIGURE 2: SIMPLIFIED BLOCK DIAGRAM OF EXPERIMENTAL APPARATUS

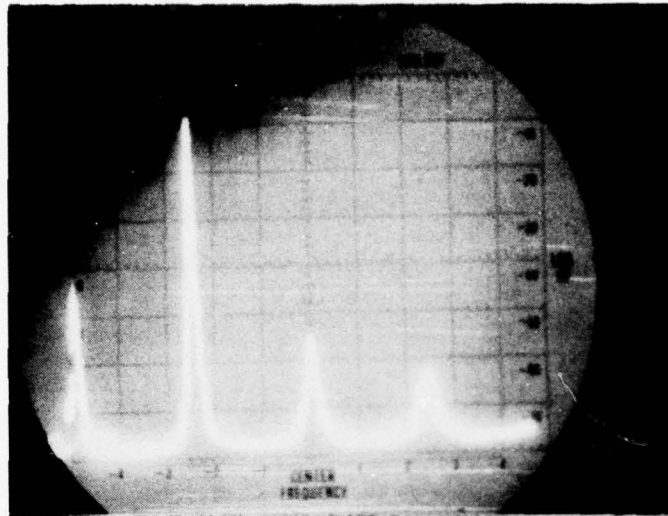


FIGURE 3: FREQUENCY SPECTRUM OF ELECTROSTATIC ION CYCLOTRON WAVE
 First Peak is the Zero Reference, Center Frequency = $\omega_s/2\pi = 228$ KHz, $P = 1.2\mu$, $f_o = 9.23$ GHz, $P_1 = 173$ W (cw), Linear Vertical Scale, 90 KHz/Division Horizontal Scale

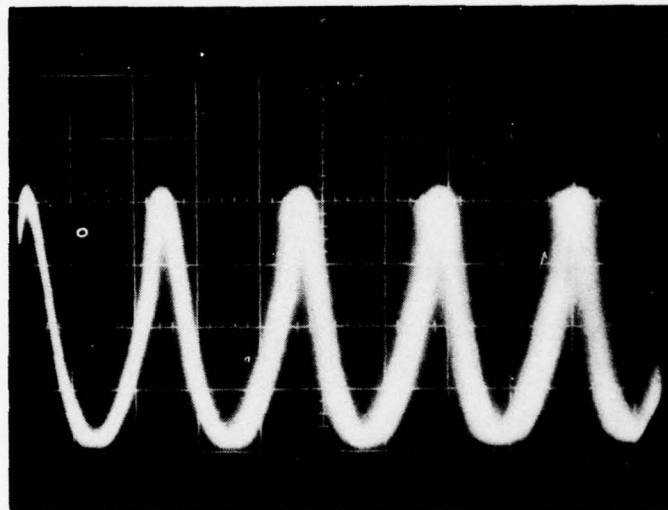


FIGURE 4: TIME DOMAIN BEHAVIOR OF ELECTROSTATIC ION CYCLOTRON WAVE
 $P = 1.2\mu$, $f_o = 9.23$ GHz, $P_1 = 173$ W (cw), Horizontal Scale = $2\mu s/cm$, Vertical Scale = $.5$ V/cm

In order to parametrically excite the electrostatic ion cyclotron waves efficiently, the external dc magnetic field is suitably adjusted such that the frequency of the pump field is near or just above the harmonic of electron cyclotron frequency. We find that in the HCD device, the plasma is very unstable due to the existence of various types of low frequency unstable modes which are suspected to be: resistive drift, ion acoustic, and electrostatic ion cyclotron instabilities. It is believed that the energy source responsible for the onset of these instabilities must come from the excess of the free energy contained in the plasma not at thermodynamic equilibrium. In this regard, we find the possible deviations from equilibrium occurring in the velocity space are due to the mirror field in the source region, and not to the configuration space. This conclusion follows from the fact that all the low frequency unstable modes disappear after the source plasma is turned off completely.

Strongly enhanced signals at the acoustic wave frequencies are observed only when the pump power exceeds a threshold level. This is the characteristic of parametric excitation. With the background gas pressure readjusted to about 1.2μ the electrostatic ion cyclotron wave becomes most coherent in time domain as seen on a scope (Figure 4), or becomes sharpest in the frequency domain as seen on a frequency spectrum analyzer (Figure 3).

2. Measurement of Growth and Decay Times of Electrostatic Ion Cyclotron Waves

The growth and decay times of parametrically excited electrostatic ion cyclotron waves are measured as a function of microwave pump power by modulating the pump as illustrated in Figure 5. During time T_1 , the power is at level $P_1 > P_{th}$ (threshold power) such that the

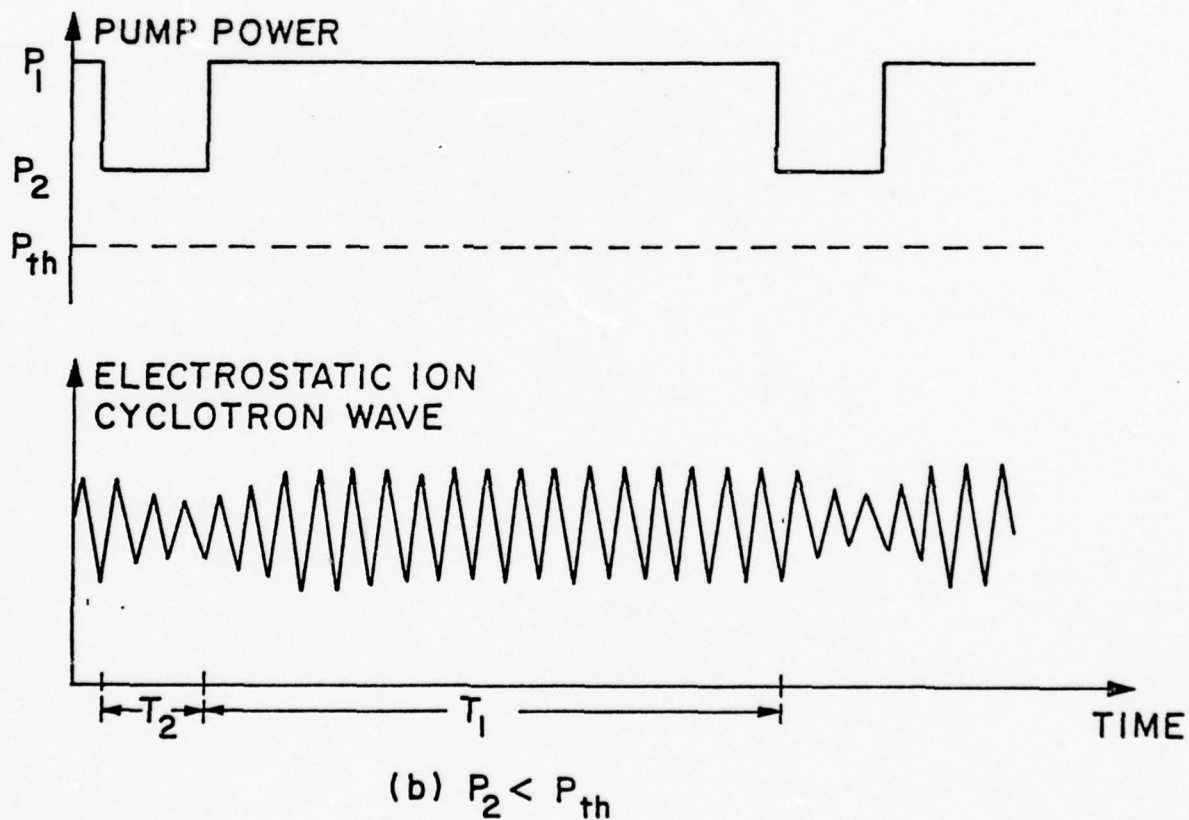
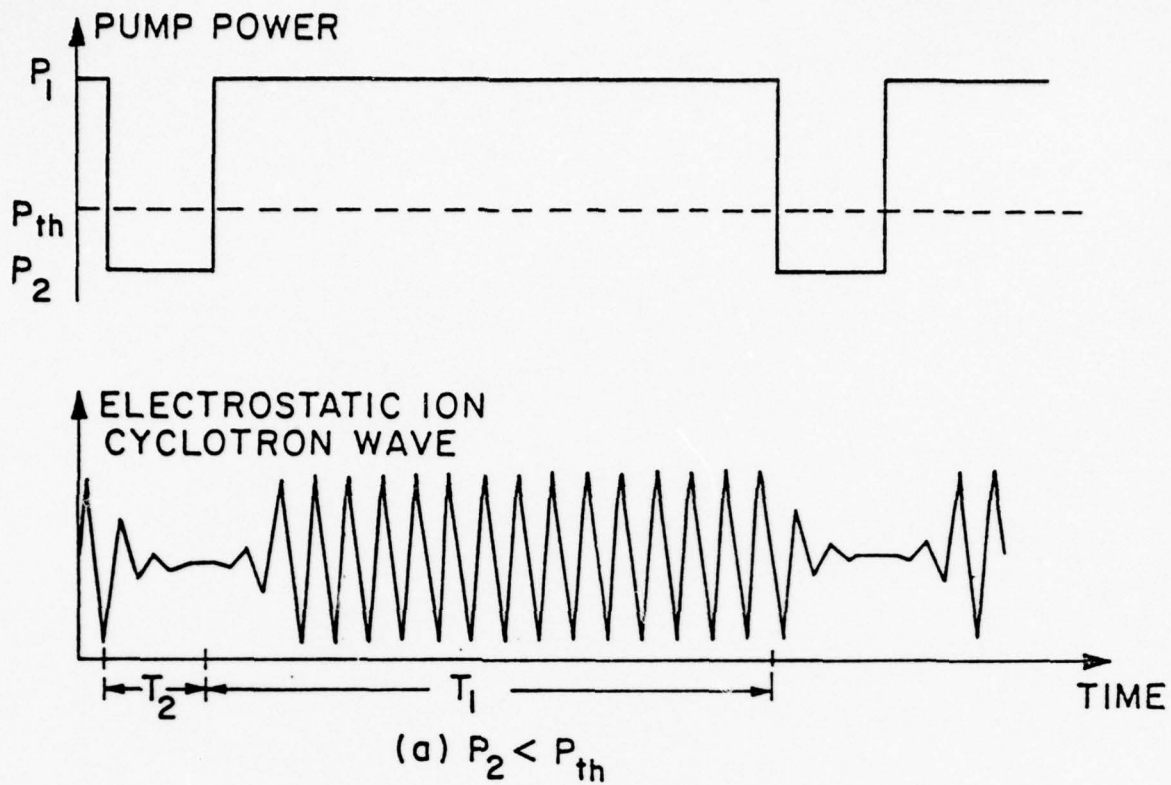


FIGURE 5: GROWTH AND DECAY OF ELECTROSTATIC ION CYCLOTRON WAVES AS A FUNCTION OF PUMP POWER

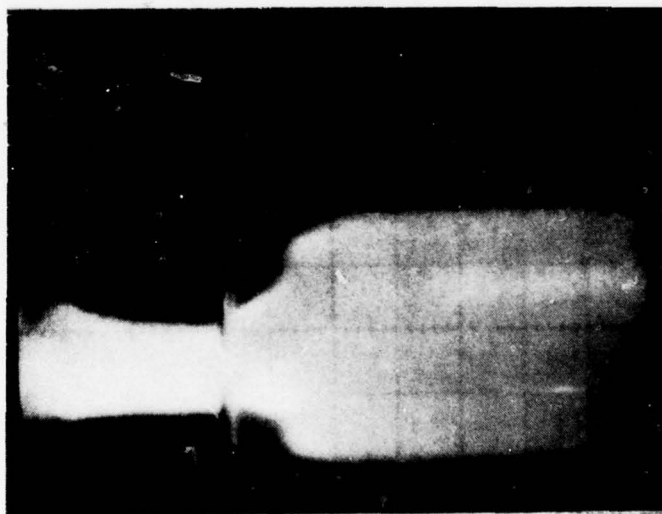
electrostatic ion cyclotron wave grows to a finite amplitude as shown in the sketch. At the end of time T_1 and the beginning of T_2 , the power is switched to a new level P_2 . If $P_2 < P_{th}$, the wave decays to zero during time T_2 , providing that T_2 is of sufficient duration, as shown in Figure 5a. If $P_2 > P_{th}$ and $P_1 > P_2$, the wave decays during T_2 from the amplitude excited by P_1 to a new nonzero steady state amplitude corresponding to P_2 as shown in Figure 5b. Modulating the power as described, the growth and decay times, and the amplitude of the electrostatic ion cyclotron wave, are measured as a function of P_2 , for both below and above the threshold. The total time $T_1 + T_2$ of the microwave signal is approximately 2.3 milliseconds and T_1 is typically 75% of this period.

Photographs containing many traces of the electrostatic ion cyclotron waves are used to obtain the growth and decay time. Since the plasma beam is isolated by a large vacuum chamber, the signal detected by the optical system (through optical fiber bundles to the photomultiplier tube) is too weak to overcome the inherent noise of the photomultiplier tube. Due to this, a Langmuir probe to detect the electrostatic ion cyclotron waves is used. The results thus obtained are fairly good even with the slight difficulty of synchronizing the excited signal with the modulating signal. This probe detection technique is also used to measure the steady state amplitude of the potential oscillation, thus enabling us to obtain information on the saturation mechanism.

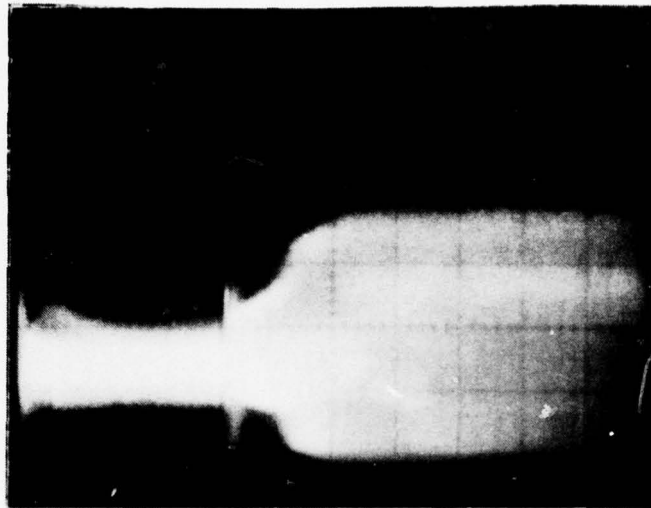
A series of photographs containing the average growth and decay of the electrostatic ion cyclotron wave is shown in Figure 6 where the pump power is modulated as in Figure 5b with $T_1 = 1.7$ ms and $T_2 = .6$ ms and both P_1 and P_2 are above the threshold level. First, P_1 is set to a level such that the instability is most coherent with the



(a) $P_2 = 83 \text{ W}$, $P_1 = 173 \text{ W}$



(b) $P_2 = 75.5 \text{ W}$, $P_1 = 173 \text{ W}$



(c) $P_2 = 65.5 \text{ W}$, $P_1 = 173 \text{ W}$

FIGURE 6: DECAY AND GROWTH OF ELECTROSTATIC ION CYCLOTRON WAVE FROM ONE STEADY STATE AMPLITUDE INTO ANOTHER

$P = 1.2 \mu$, $f_0 = 9.23 \text{ GHz}$, Horizontal Scale = $.2 \text{ ms/cm}$

$T_2 = .6 \text{ ms}$, $T_1 = 1.7 \text{ ms}$

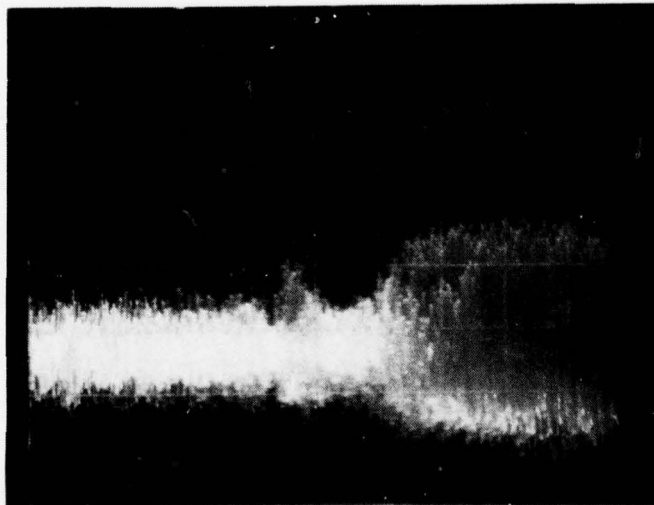


FIGURE 7: PHOTOGRAPH SHOWS THAT THERE IS A TRANSITION PERIOD BEFORE WAVE REALLY STARTS TO GROW

lowest possible neutral gas pressure. We then progressively increase the voltage amplitude of the modulating signal (which is applied to the PIN diode switch) to lower the P_2 level, and the series of photographs are taken with the scope trace triggered to start when the power is switched to P_2 level. The initial decay rate of the instability, when power is switched from P_1 to P_2 , is difficult to be calculated because of its strong dependence on the initial amplitude of the instability; therefore, the average decay rate as shown in Figure 8 is calculated by averaging over the e-folding time, i. e., the time it takes for the amplitude decreases to $1/e$ of its initial value. Figure 6 also shows the existence of a transient before the wave starts to grow. This may be explained by noting that during both T_1 and T_2 of the growth experiments, the electron-neutral collision frequency is much larger than the average decay rate of the electrostatic ion cyclotron wave shown in the Figure 8. During T_2 the electron temperature of the plasma is lowered because of decrease in pump power, and at the end of T_2 , the electron temperature rises back quickly to its original level, but it takes finite time for the frequency of the instability to switch back. A typical multiple trace photograph shown in Figure 7 clearly displays this kind of delay phenomenon. Nevertheless, the linear relation between the initial growth rate γ and P_2 is clearly demonstrated in Figure 9. The curve in Figure 8 shows that as P_2 progressively decreases, (as noted in the series of photographs) the decay rate increases. Eventually P_2 reaches a power level such that it takes the wave the period T_2 to decay to zero as shown in Figure 10, and this corresponds to the threshold power.

Decreasing T_2 and increasing the total period $T_1 + T_2$ (i. e., decreasing the modulation frequency) of the microwave signal, it is possible

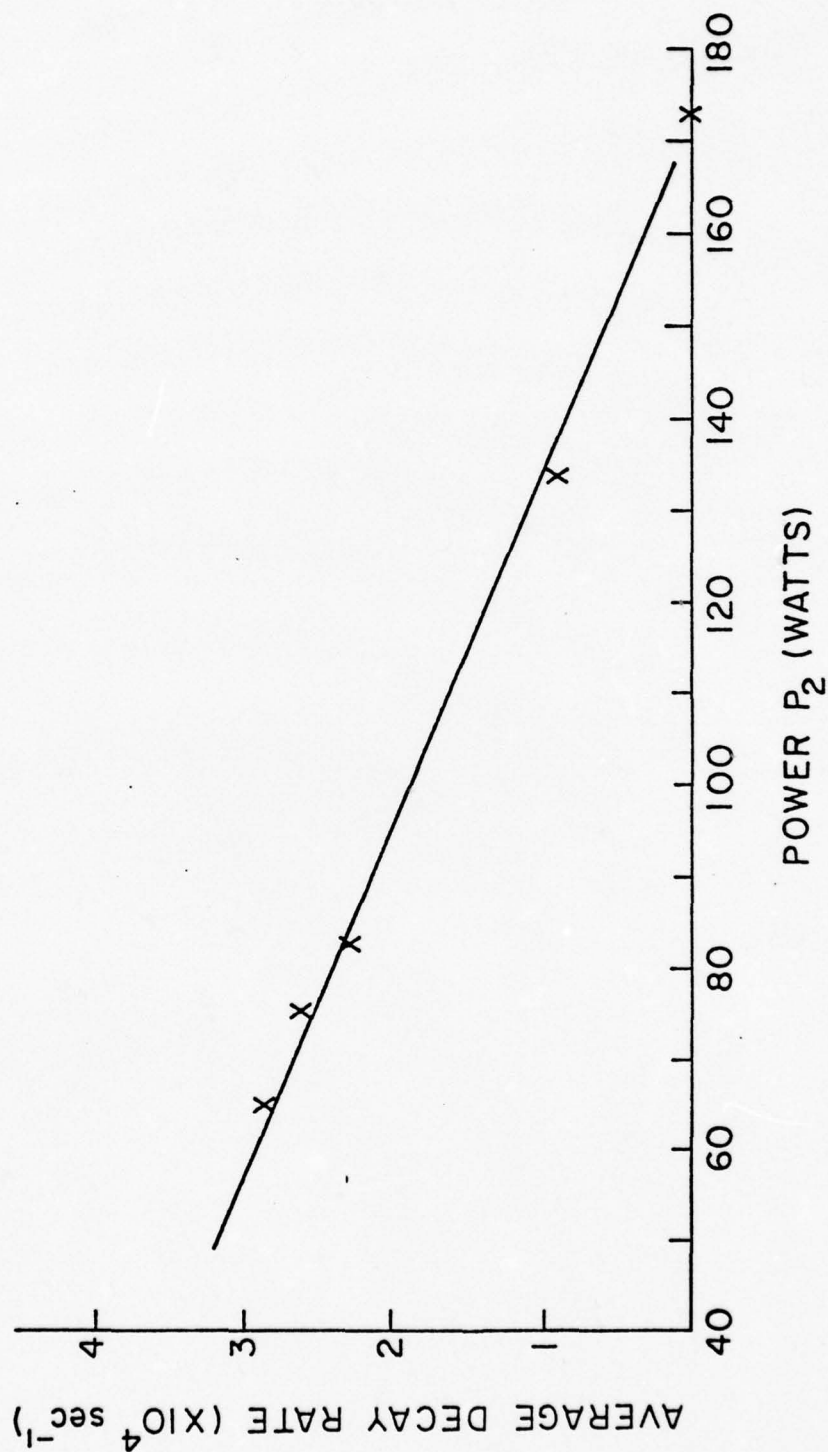


FIGURE 8: AVERAGE DECAY RATE OF ELECTROSTATIC ION CYCLOTRON WAVE AS A FUNCTION OF POWER P_2 WITH $P_1 = 173 \text{ W}$ FIXED
 $P = 1.2 \mu$ $f_o = 9.23 \text{ GHz}$.

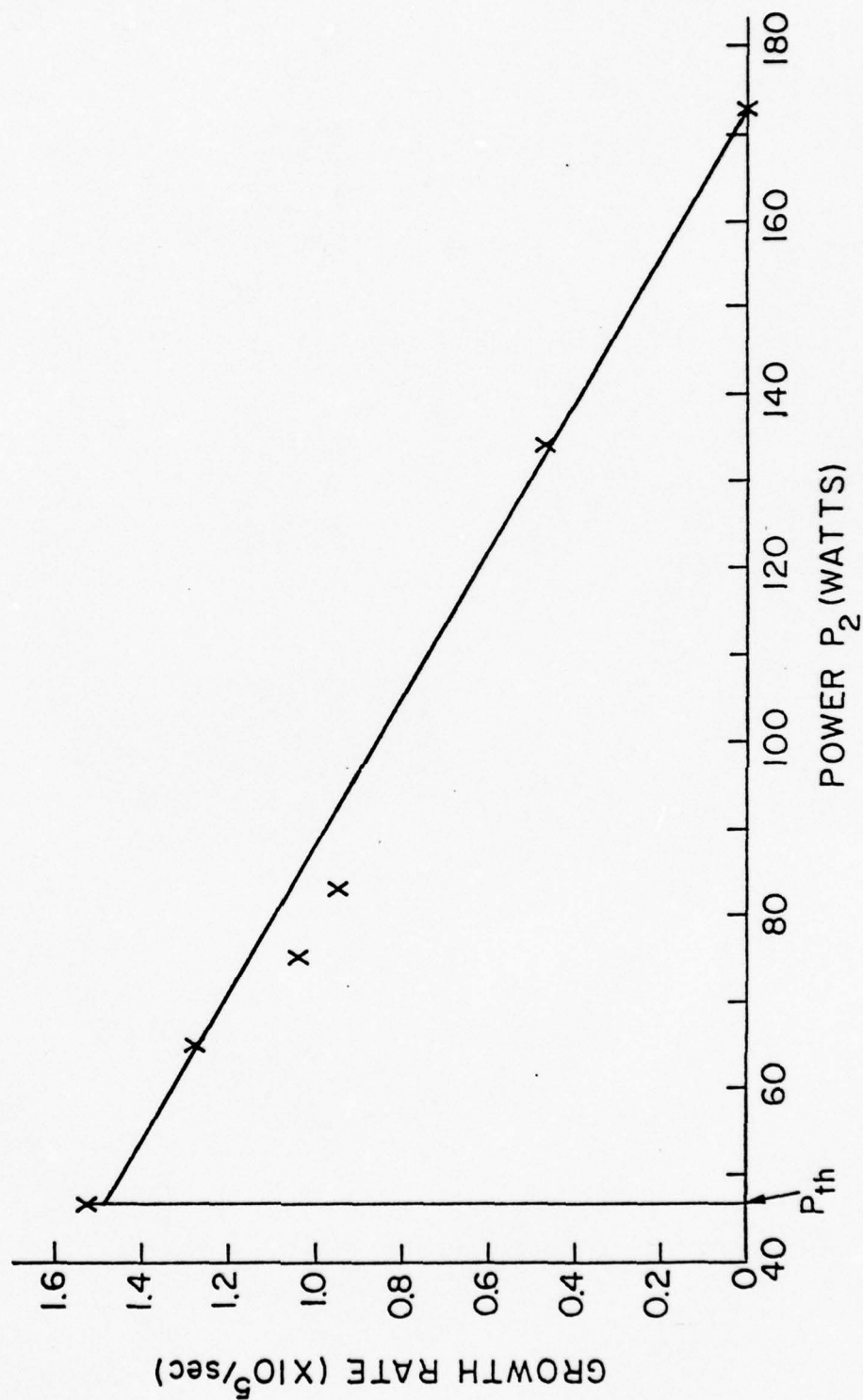


FIGURE 9: INITIAL GROWTH RATE OF ELECTROSTATIC ION CYCLOTRON WAVE FROM ONE STEADY STATE AMPLITUDE TO ANOTHER AS A FUNCTION OF POWER P_2 : $P_1 = 173$ W, $P = 1.2 \mu$, $f_o = 9.23$ GHz

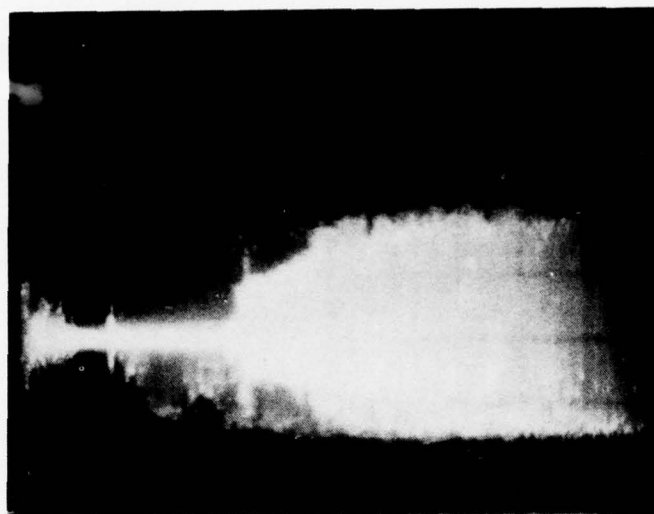
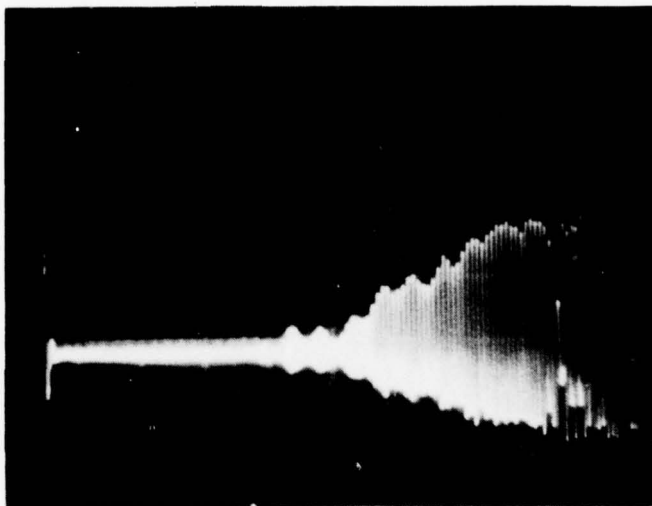


FIGURE 10: DECAY OF ELECTROSTATIC ION CYCLO-
TRON WAVE FROM STEADY STATE AM-
PLITUDE INTO NOISE FOR PUMP POWER
JUST BELOW THRESHOLD LEVEL

$P_2 = 47.1 \text{ W}$, $P_1 = 141 \text{ W}$, $T_2 = .2 \text{ ms}$,
 $T_1 = 2.1 \text{ ms}$, Horizontal Scale = $.1 \text{ ms/cm}$

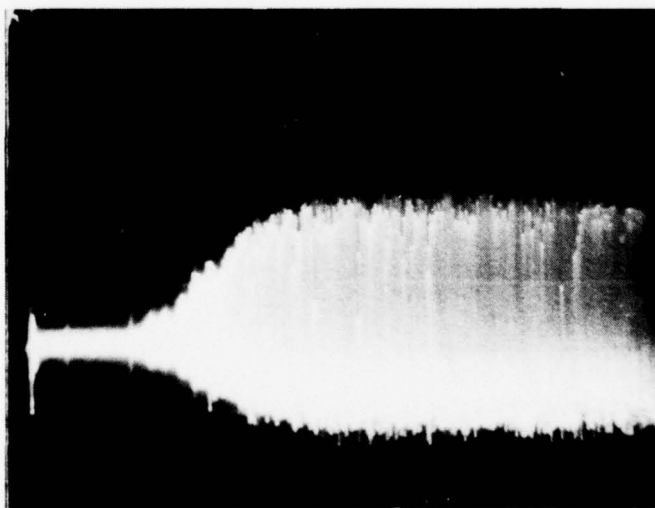
to lower the power level P_2 to almost zero. Single and multiple traces photographs shown in Figure 11 display the growth (and decay) of the electrostatic ion cyclotron wave as power P_2 is varied from 0 watt to 173 watts. Only a portion of the total period is shown in the photograph. The wave starts to grow only with the pump power exceeding the threshold level, and it becomes an eigenmode of the collisional plasma. During the initial buildup of the potential oscillation, the energy density arising from spontaneous emission of the background plasma is comparable to the energy density produced by the parametric interaction. Therefore, to determine the initial growth rate we must calculate the growth time only after the wave has a small finite amplitude. This value is also shown in Figure 9, and is consistent with the theoretical calculation from equation (4.17).

There are two kinds of damping in our system. Linear or natural damping occurs when the pump is below the threshold level. Once the threshold level is exceeded, the amplitude of the instability would theoretically grow to infinity. However, due to the nonlinear damping, the wave always reaches a saturated state. Therefore, the nonlinear damping would exactly balance the initial growth rate of the wave at that particular power level. If the pump power is suddenly reduced to zero as in the case in Figure 11b, its initial decay rate must be equal to the sum of the linear damping rate and the initial growth rate of Figure 11a. Hence we have a linear damping rate of about $0.6 \times 10^5 \text{ sec}^{-1}$ for the electrostatic ion cyclotron waves; this value is consistent with the value calculated from the tail of the decay diagram. From this value, we can conclude that the linear damping mechanism is due to ion-neutral collisions with the ion temperature of about 0.6 eV. This value of ion temperature



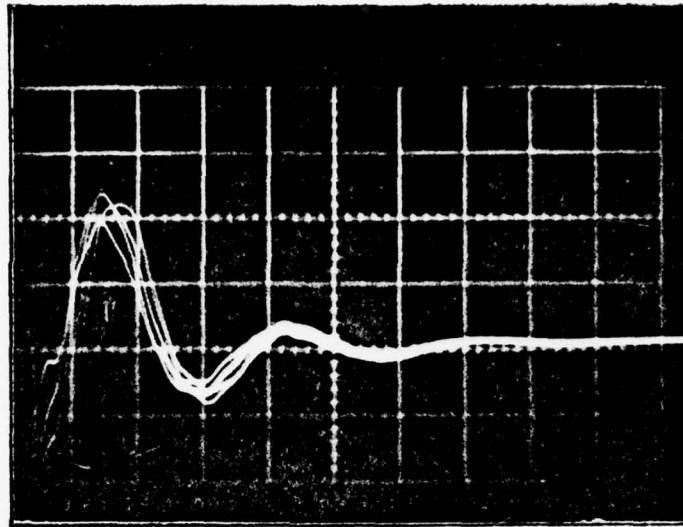
(a) SINGLE-SHOT PHOTOGRAPH

$P_2 = 0 \text{ W}$, $P_1 = 173 \text{ W}$, $P = 1.2 \mu$,
Horizontal Scale = $50 \mu\text{s/cm}$



(b) MULTIPLE-TRACE PHOTOGRAPH

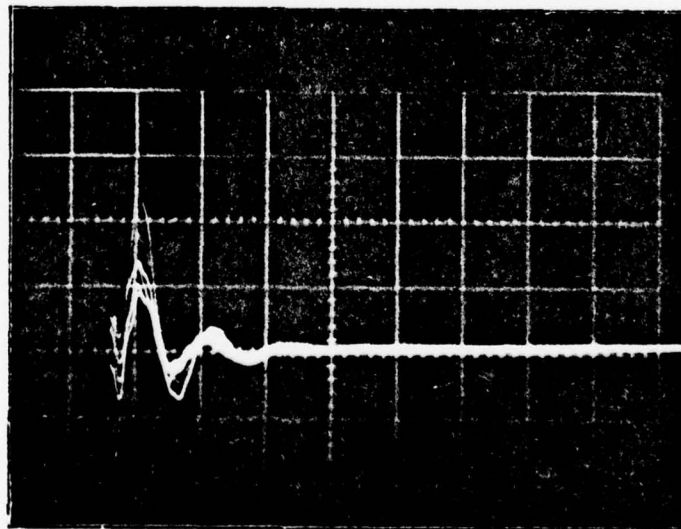
$P_2 = 0 \text{ W}$, $P_1 = 173 \text{ W}$, $P = 1.2 \mu$
Horizontal Scale = $.1 \text{ ms/cm}$



(c) MULTIPLE-TRACE PHOTOGRAPH

$P_1 = 173 \text{ W}$, $P_2 = 0 \text{ W}$, $P = 1.2 \mu$

Horizontal Scale = $2 \mu\text{s/cm}$



(d) $P_1 = 173 \text{ W}$, $P_2 = 0 \text{ W}$, $P = 1.2 \mu$

Horizontal Scale = $5 \mu\text{s/cm}$

FIGURE 11: GROWTH AND DECAY OF ELECTROSTATIC ION CYCLOTRON WAVE FOR $P_1 = 173 \text{ W}$ AND $P_2 = 0 \text{ W}$

has been verified experimentally in Kristal's²⁶ thesis by using a Fabry-Perot interferrometer.

3. Frequency of Electrostatic Ion Cyclotron Wave as a Function of Pump Power

The frequency shift of the electrostatic ion cyclotron wave due to pump power has also been investigated. These experiments are conducted with cw microwave excitation, and the frequency is measured on the low frequency spectrum analyzer.

Electrostatic ion cyclotron frequency is shown as a function of power in Figure 12 for a fixed pressure. As shown in Table 1, the frequency shift is linearly proportional to the change of electron temperature with some discrepancy. This can be explained from the linear parametric theory, which indicates a frequency shift due to finite growth rate. After substituting all the known parameters into equation (4.20), this discrepancy becomes more evident. However, with a minor correction, the linear relationship between the frequency shift and electron temperature change is clearly shown in Figure 13.

Electron density with the presence of the pump wave is also measured by using the probe technique. As shown in Figure 14 the electron density at the center of the plasma column decreases as the instability increases. But the pump power increases over some level, the ionization rate may cover the enhanced diffusion rate, causing the density to increase again.

4. Summary of Experimental Parameters

Table 2 summarizes the basic experimental parameters. The values given are for a magnetic field of 1.64 kilograms and for a pressure of 1.2μ

TABLE 1 -- EXPERIMENTAL AND THEORETICAL DATA IN SEVERAL PUMP POWER LEVELS										
Pump Power P_1 (watts)	104.5	132.6	144.6	161	193	237	305	498		
Frequency of electrostatic ion cyclotron wave f_s ($\times 10^3$ Hz)		217.4	220.3	226	232.6	243.9	253.2	285.7		
Frequency shift with respect to the frequency of 132.6 watts Δf_s ($\times 10^3$ Hz)			2.9	8.6	15.2	26.5	35.8	68.3		
Electron temperature T_e (eV)	5.58	5.85	6	6.35	6.63	7.13	7.13	7.9		
Frequency shift due to electron temperature increase $\Delta f_1 = \frac{k^2 \Delta T_e}{8\pi^2 f_s M_i 10^3} (\times 10^3 \text{ Hz})$			2.49	8.3	12.87	21.17	21.17	34.03		
Frequency shift due to finite initial growth rate $\Delta f_2 = \frac{\Gamma_s^2}{8\pi^2 \times 10^3 f_s} \left[\frac{E_o^2}{E_c^2} - 1 \right] (\times 10^3 \text{ Hz})$		1.9	2.32	3.11	4.39	6.83	11.6	31.75		
$\Delta f_1 + \Delta f_2 - 1.9 (\times 10^3 \text{ Hz})$			2.91	9.35	15.36	26.1	30.9	63.9		
plasma density $n_e = n_i = n_o (\times 10^{12}/\text{cm}^3)$.88	.82	.77	.79	.80	.80	.82	.87		

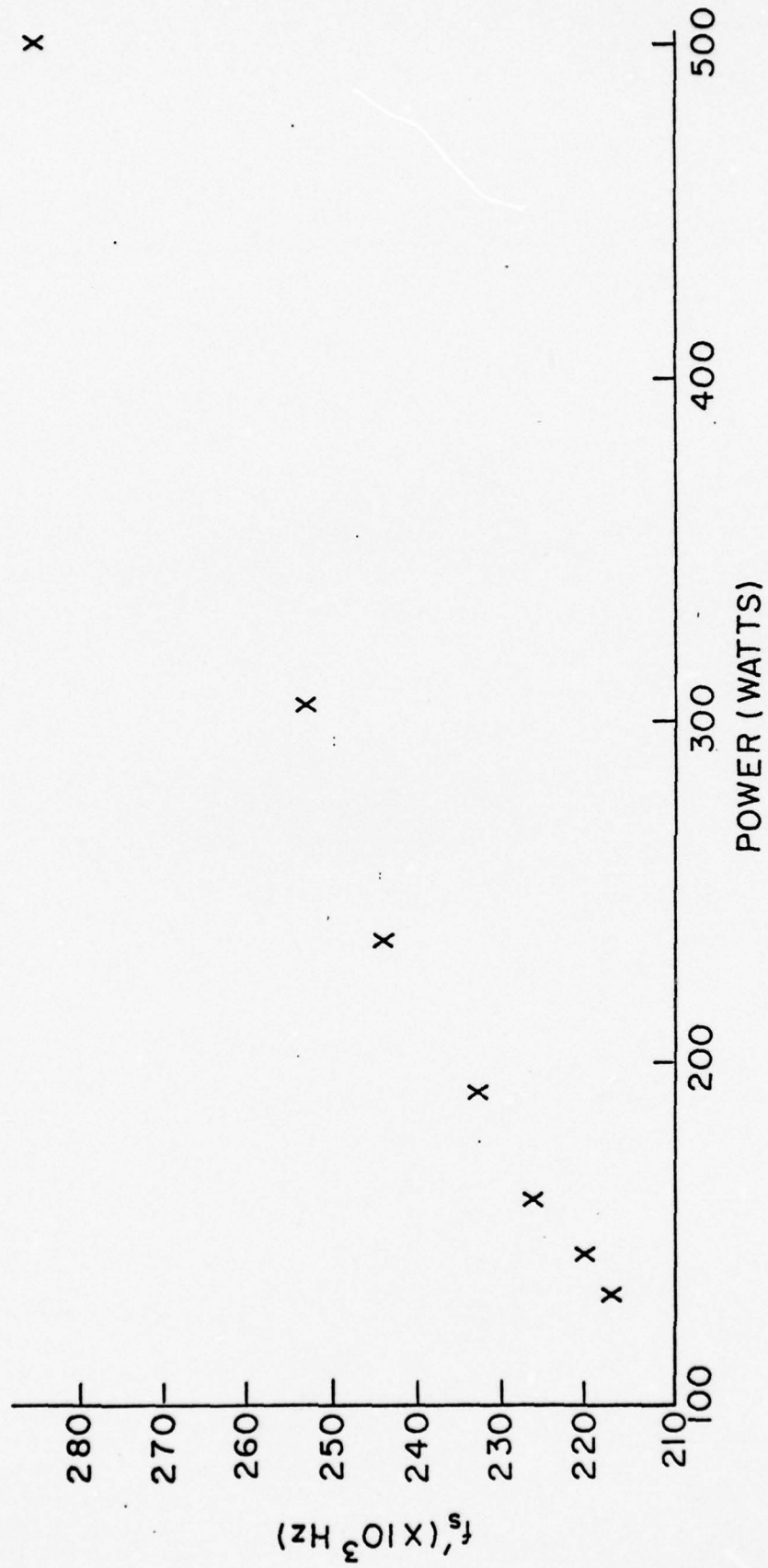


FIGURE 12: FREQUENCY OF ELECTROSTATIC ION CYCLOTRON WAVE AS A FUNCTION OF PUMP POWER

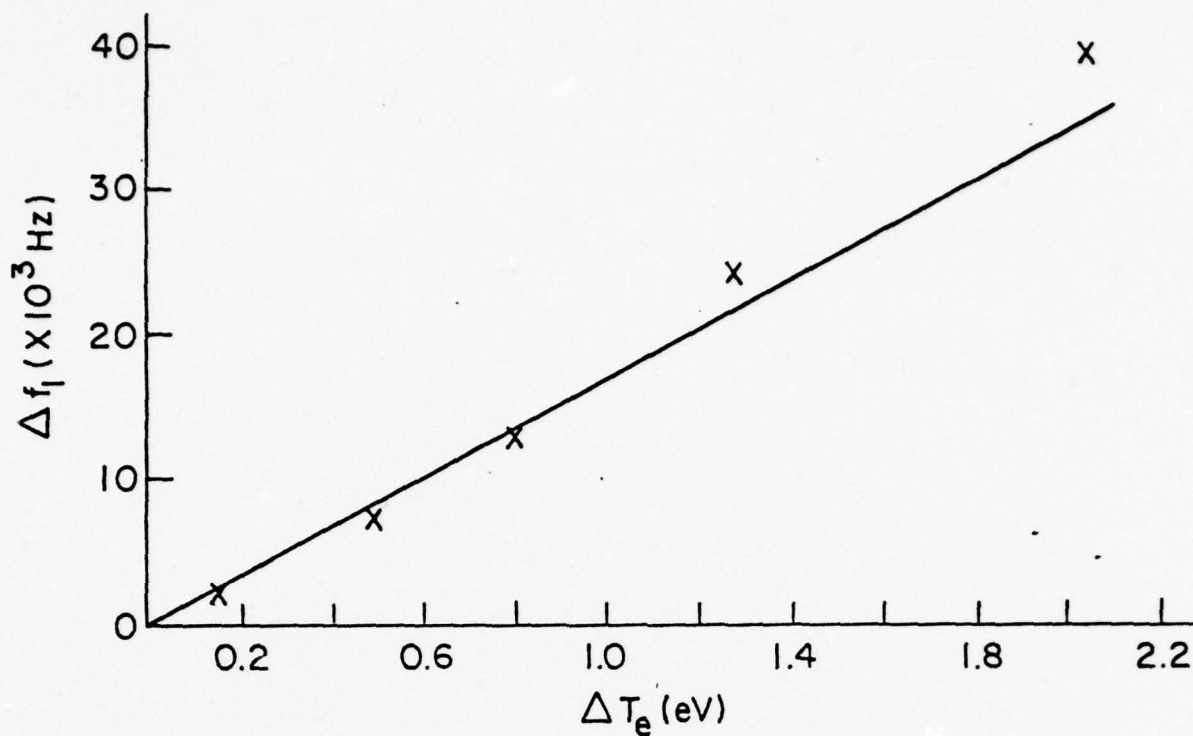


FIGURE 13: MEASURED ELECTROSTATIC ION CYCLOTRON FREQUENCY SHIFT AS A FUNCTION OF ELECTRON TEMPERATURE CHANGE

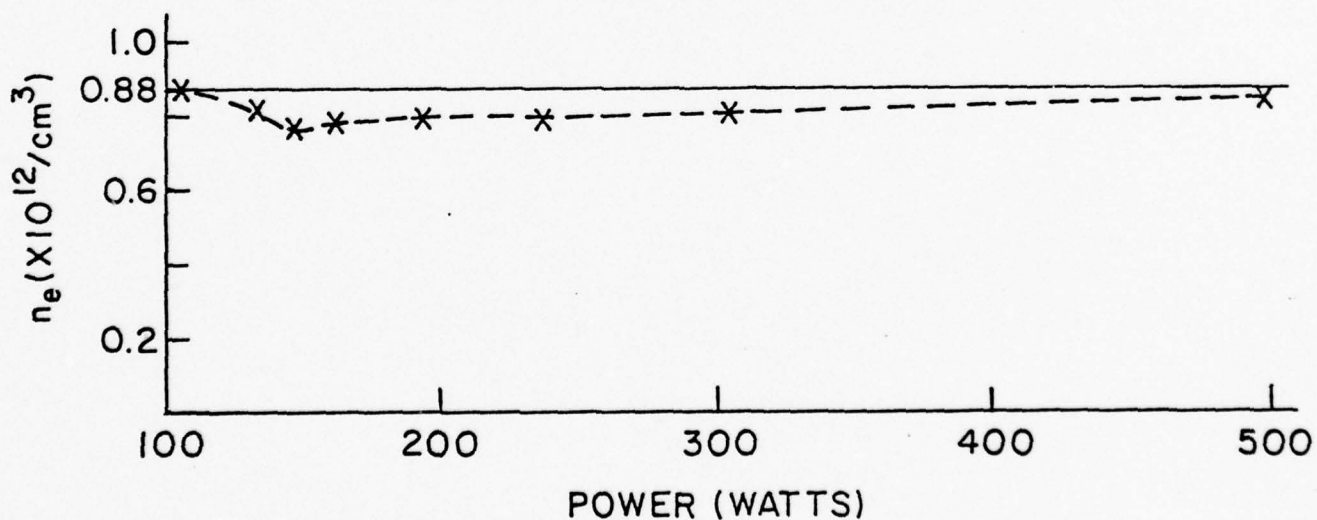


FIGURE 14: PLASMA DENSITY AS A FUNCTION OF PUMP POWER

TABLE 2 - EXPERIMENTAL PARAMETERS

Quantity	Symbol	Value
Ion (Electron) Density	n_o	$8.8 \times 10^{11}/\text{cm}^3$
Neutral	N	$3.9 \times 10^{13}/\text{cm}^3$
Ion Temperature	T_i	0.6 eV
Electron Temperature	T_e	6 eV
Ion Cyclotron frequency $\frac{eB_o}{Mc}$	Ω_i	$3.95 \times 10^5/\text{sec}$
Electron cyclotron frequency $\frac{eB_o}{mc}$	Ω_e	$2.9 \times 10^{10}/\text{sec}$
Electrostatic Ion cyclotron frequency $(\Omega_i^2 + \frac{k^2 T_e / M}{1 + k^2 \lambda_D^2})^{1/2}$	ω_s	$1.3 \times 10^6/\text{sec}$
Second harmonic of electron cyclotron frequency	ω_ℓ	$5.8 \times 10^{10}/\text{sec}$
Pump frequency	ω_o	$5.8 \times 10^{10}/\text{sec}$
Ion-neutral collision frequency	$\nu_{in} = 2\Gamma_s$	$1.2 \times 10^5/\text{sec}$
Electron-neutral collision frequency	$\nu_{en} = 2\Gamma_\ell$	$5.2 \times 10^6/\text{sec}$
Ion plasma frequency $(\frac{4\pi n_o e^2}{M})^{1/2}$	ω_{pi}	$1.95 \times 10^8/\text{sec}$
Electron plasma frequency $(\frac{4\pi n_o e^2}{m})^{1/2}$	ω_{pe}	$5.3 \times 10^{10}/\text{sec}$
Debye length $(\frac{T_e}{4\pi n_o e^2})^{1/2}$	λ_D	$1.94 \times 10^{-3} \text{ cm}$
Radial scale length	λ_r	.48 cm
Wave number $\frac{\pi}{\lambda_r}$	k	3.3/cm
Ion Larmor radius $(\frac{8T_i}{\pi M})^{1/2} / \Omega_i$	r_{Li}	.48 cm
Electron Larmor radius $(\frac{8T_e}{\pi m})^{1/2} / \Omega_e$	r_{Le}	$.57 \times 10^{-2} \text{ cm}$
Ion thermal speed $(\frac{3T_i}{M})^{1/2}$	V_{Ti}	$2.1 \times 10^5 \text{ cm/sec}$
Electron thermal speed $(\frac{3T_e}{m})^{1/2}$	V_{Te}	$1.8 \times 10^8 \text{ cm/sec}$
Ion mass	M	$6.68 \times 10^{-23} \text{ gram}$
Electron mass	m	$0.91 \times 10^{-27} \text{ gram}$

Note that ν_{in} includes charge transfer, which accounts for about half of the total collision rate. A cross-section of $1.3 \times 10^{-14} \text{ cm}^2$ is used in the calculations.

5. Evidence of Parametric Excitation of Electrostatic Ion Cyclotron Wave

Experimental evidence and data are presented here to show that the electrostatic ion cyclotron waves are indeed parametrically excited by the microwave pump. It is found that:

- a. The polarization of the excited low frequency wave is in the direction perpendicular to the dc magnetic field.
 - b. It is a standing wave.
 - c. The excited low frequency wave is the electrostatic ion cyclotron wave.
 - d. The excited waves start to grow only when the microwave pump reaches threshold power.
 - e. Its growth and decay rates follow the theoretical linear dependence with power as predicted by parametric theories.
-
- a. First the axially movable probe is calibrated with respect to the radially movable one. Then both probes are used to measure the field strength of the wave at the same point but in two different polarizations. We find that the axial field is much smaller than the field component in the direction transverse to the dc magnetic field.
 - b. Using the radially movable probe to measure the amplitude of the transverse field as a function of the radial position, the amplitude is found to be maximum at the center and reduces to zero just outside the plasma beam. Hence we conclude this excited mode is of standing wave type, and its wave number may be calculated from the diameter of the plasma beam.
 - c. To support the contention that the excited low frequency wave is electrostatic ion cyclotron wave, we note that the observed frequency is almost independent of the plasma density and dc magnetic field; therefore the possibility of exciting lower hybrid wave or harmonics of ion cyclotron wave is excluded. We also note that the observed electrostatic ion cyclotron frequency matches the one determined by the linear dispersion relation with known wavenumber, electron temperature, ion mass and dc magnetic field. Since the linear dispersion relation of the electrostatic ion cyclotron wave is

$$\omega^2 = \Omega_i^2 + k^2 \frac{T_e}{M_i} / 1 + k^2 \lambda_D^2$$

the frequency shift due to the change of electron temperature may be expressed as

$$\Delta f = \frac{k^2}{4\pi\omega M_i} \Delta T_e$$

This linear relationship has been shown in Figure 13.

- d. Multiple trace photographs shown in Figure 6 and Figure 10 display both decay and growth phenomena of the electrostatic ion cyclotron wave. Decay waves have finite steady state amplitude only for pump powers above a threshold.
- e. Possibly the most convincing evidence of parametric excitation of the electrostatic ion cyclotron wave lies in the main theme of this effort, i. e., the growth and decay rates of the excited ion acoustic waves are linearly related to pump power as shown in Figures 8 and 9.

6. Simplified Theoretical Explanation

The linear parametric theory derived in the preceding chapter gives us a consistent prediction of threshold power and initial growth rate. Since it does not include the saturation effects, it fails to describe the growth or decay of the unstable wave from one saturated amplitude to another. Nevertheless, the result given in Eq. (4.19) leads us to propose a phenomenological model for wave growth and decay in the presence of saturation effects as the pump power is near threshold. The amplitude A of the electrostatic ion cyclotron wave may be governed phenomenologically as

$$\frac{dA}{dt} = \Gamma_s \left[\frac{E_o^2}{E_c^2} - 1 \right] A - c_3 A^{n+1} \quad (5.1)$$

where E_o^2 is the square of the electric field in the plasma produced by the pump and E_c^2 is the square of the threshold field. Γ_s is the linear

damping rate and $c_3 A^n$ is the phenomenological nonlinear damping rate and n is an integer of unknown value which may be determined from the experimental data.

The exact solution of (5.1) for $n > 0$ is

$$A(t) = \frac{A_0 e^{yt}}{\left[1 + \frac{A_0^n c_3}{y} (e^{nyt} - 1) \right]^{1/n}} \quad (5.2)$$

where $y = \Gamma_s \left[\frac{E_0^2}{E_c^2} - 1 \right]$ is the linear growth (or decay) rate and $A_0 = A(0)$

is the initial amplitude of the wave.

$$\text{As } t \rightarrow \infty$$

$$A^n(\infty) = \frac{y}{c_3} = \frac{\Gamma_s \left(\frac{E_0^2}{E_c^2} - 1 \right)}{c_3} > 0 \quad \text{for } y > 0 \quad (5.3)$$

and

$$A(\infty) = 0 \quad \text{for } y < 0 \quad (5.4)$$

Hence the value of n can be experimentally determined by plotting the n^{th} power of the steady state amplitude of the electrostatic ion cyclotron wave as a function of pump power for $y > 0$ as shown in Figure 15. With $n = 2$, this graph becomes linear, and is in agreement with the prediction of (5.3). Setting $n = 2$ in (5.2) and (5.3), we obtain

$$A(t) = \frac{A_0 e^{yt}}{\left[1 + \frac{A_0^2 c_3}{y} (e^{2yt} - 1) \right]^{1/2}} \quad (5.5)$$

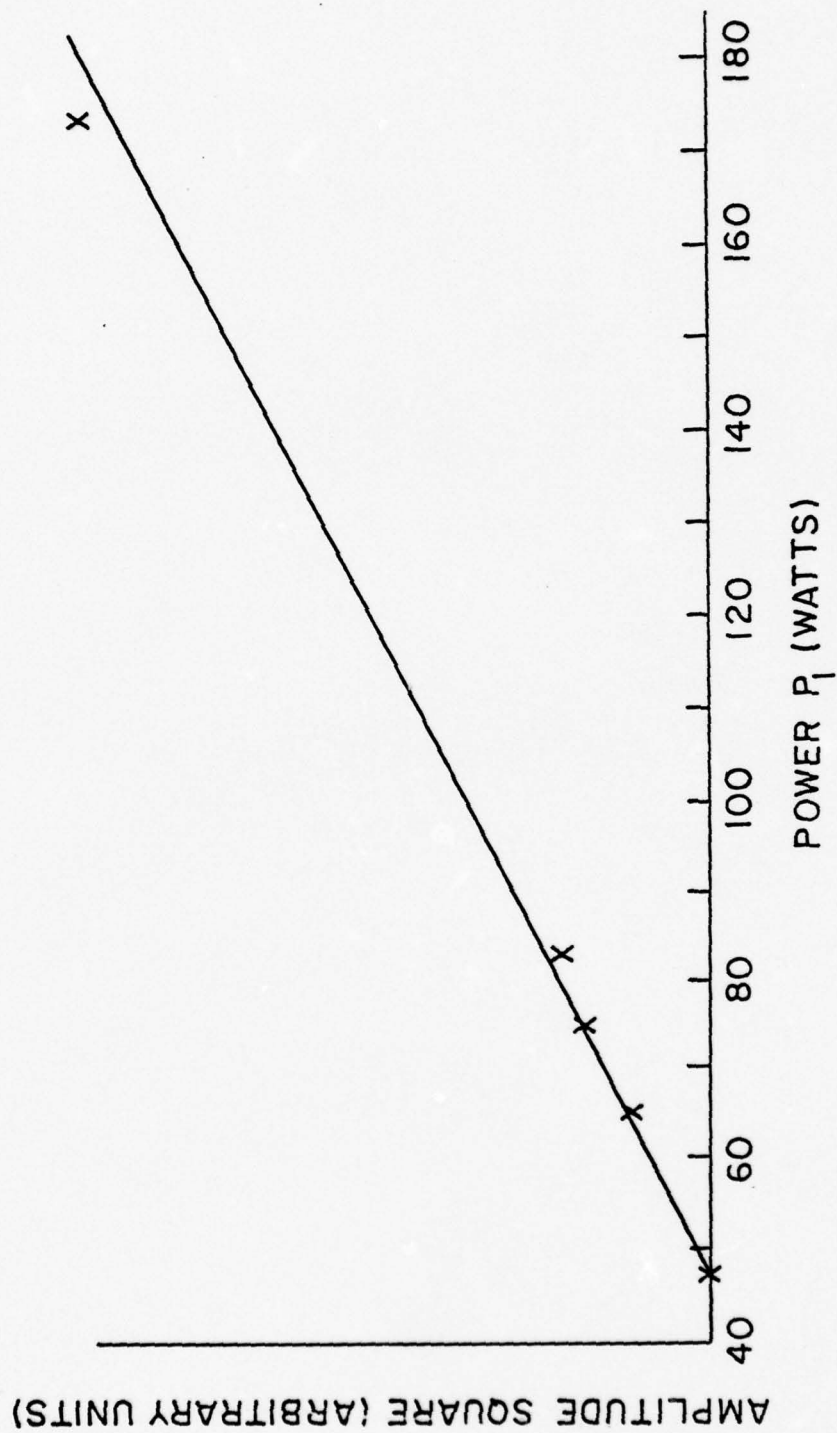


FIGURE 15: SQUARE OF THE SATURATED AMPLITUDE OF THE ELECTRO-STATIC ION CYCLOTRON WAVE AS A FUNCTION OF PUMP POWER FOR POWER ABOVE THRESHOLD.

and

$$A(\infty) = \left(\frac{y}{c_3} \right)^{1/2} = \left[\frac{\Gamma_s \left(\frac{E_o^2}{E_c^2} - 1 \right)}{c_3} \right]^{1/2} \quad \text{for } y > 0 \quad (5.6)$$

respectively.

Now we proceed to explain the experimental results shown in Figures 8 and 9 by using (5.1).

Assuming the pump power is switched from P_1 to P_2 (or P_2 to P_1) as in the case shown in Figure 5b, then the wave decays (or grows) from original steady state amplitude $A(0)$ to another steady state amplitude $A(\infty)$.

Rewriting Eq. (5.1) as

$$\frac{dA}{dt} = \left[\Gamma_s \left(\frac{E_1^2}{E_c^2} - 1 \right) - c_3 A^2 \right] A = \left[\Gamma_s \left(\frac{E_1^2 - E_2^2}{E_c^2} \right) + c_3 (A_o^2 - A^2) \right] A \quad (5.7)$$

for the growth case

where E_1 and E_2 are the field corresponding to P_1 and P_2 respec-

tively, and $A_o^2 = \frac{\Gamma_s \left(\frac{E_2^2}{E_c^2} - 1 \right)}{c_3}$ is the steady state amplitude of electro-

static ion cyclotron wave at P_2 power level, and

$$\frac{dA}{dt} = \left[\Gamma_s \left(\frac{E_2^2}{E_c^2} - 1 \right) - c_3 A^2 \right] A = - \left[\Gamma_s \left(\frac{E_1^2 - E_2^2}{E_c^2} \right) + c_3 (A^2 - A_o^2) \right] A \quad \text{for} \quad (5.8)$$

decay case

where $A_o^2 = \frac{\frac{E_1^2}{E_c^2} - 1}{c_3} \Gamma_s$ is the steady state amplitude of electrostatic

ion cyclotron wave at P_1 power level.

Then Eqs. (5.7) and (5.8) show that the initial growth rate (or decay rate) is linearly proportional to the power level P_2 .

VI. NONLINEAR SATURATION MECHANISM

1. Introduction

We have so far considered only linear parametric theory and a phenomenological nonlinear equation which describes the low frequency unstable wave. Since saturation phenomenon is always present in experiments, an important question must be raised in order to describe the kind of nonlinear damping mechanisms which cause the instabilities to saturate. There have been earlier attempts to describe the mechanism as due to induced scattering^{27, 28}, and cascading^{29, 30, 31} of the side band into even lower frequency waves and resonance broadening³². Other possible mechanisms include pump depletion and quasi-linear effects (i. e., heating). There is no generalization to be applied, because the nonlinear effects may vary for different experimental systems. As an example, if one nonlinear damping mechanism, among other competing phenomena, becomes dominant and cause to saturate before the pump depletion, then we must rule out pump depletion due to priority, or if the unstable wave is coherent, then we must reject the mechanism due to the cascading of the sideband. Therefore, the dominance among different mechanisms depends greatly on the geometry of the individual system, and the mode-types involved. Disregarding the effect of inhomogeneity, systems may be classified into three classes:

(1) Infinite plasma

When the dimensions of the plasma is much larger than the wavelength of the instabilities, boundary conditions need not be considered. Therefore, the excited modes are traveling waves, and the spectrum may be strongly broadened. In such a case, the saturation of instabilities may be due to the pump being depleted to the threshold level. Another possibility

is the interaction of the excited large-amplitude oscillations among themselves, causing a continuous flow of energy toward the large wave number region. This oscillation energy is eventually dissipated into heat by collisional damping, or via collective effects. The threshold level of the instability is thus increased, and a nonlinear saturated state may eventually be reached.

(2) Bounded plasma with sheath

If the spectra of the excited modes are sharply defined because of the confines of the boundary, the potential oscillations of the low frequency waves may carry the ion bunch into the sheath region. Therefore, recombination of ion bunches at the sheath may be the dominant nonlinear damping mechanism in this case. Since the recombination rate is linearly proportional to the density of the ion bunch, this nonlinear damping process corresponds to the $n=1$ case.²⁴

(3) Bounded plasma without sheath

Excited modes are of the standing wave type, producing a well defined frequency spectra. From supercritical stability theory, anomalous diffusion of the plasma due to the low frequency unstable oscillations may be one of the nonlinear damping mechanisms, which corresponds to $n=2$ case. Another possible mechanism is the nonlinear harmonic (or subharmonic) generation, with second harmonic generation corresponding to $n=2$ case.

2. Theory

In this section the description of the nonlinear damping mechanisms for case (3), bounded plasma without sheath, will be given. The experimental results in Chapter V show that (a) a density decrease in the central portion of the plasma column coincides with an increase in amplitude of

the instability. When pump power is increased over a certain level, the ionization rate would cover the enhanced diffusion rate, causing the density to increase. (b) Harmonics of the instability are also excited. The amplitude relative to that of the fundamental is small if the pump level is low, but increases with an increase in pump power.

It should be pointed out that since the excited mode is an electrostatic ion cyclotron wave, these harmonics are still in the resonance region, and they have the same linear damping rate as that of the fundamental mode. Neglecting the nonlinear damping of the harmonics, the nonlinear damping rate of the fundamental instability due to its harmonic generation may be defined as follows

$$2\Gamma_{s1}^N \left| \delta E_s(\underline{k}, \omega_s) \right|^2 \Delta\omega_{s1} = 2\Gamma_s \left\{ \left| \delta E_s(2\underline{k}, 2\omega_s) \right|^2 \Delta\omega_{s2} + \left| \delta E_s(3\underline{k}, 3\omega_s) \right|^2 \Delta\omega_{s3} + \dots \right\} \quad (6.1)$$

or

$$\Gamma_{s1}^N = \Gamma_s \left\{ \frac{\Delta\omega_{s2}}{\Delta\omega_{s1}} \left| \frac{\delta E_s(2\underline{k}, 2\omega_s)}{\delta E_s(\underline{k}, \omega_s)} \right|^2 + \frac{\Delta\omega_{s3}}{\Delta\omega_{s1}} \left| \frac{\delta E_s(3\underline{k}, 3\omega_s)}{\delta E_s(\underline{k}, \omega_s)} \right|^2 + \dots \right\} \quad (6.2)$$

where the left hand side of (6.1) is the effective instability energy depletion rate, and the right hand side is the damping rate of the energy of the excited harmonics in steady state. $\Delta\omega_{si}$ ($i=1, 2, 3, \dots$) is the bandwidth of each spectrum. Experimental observations indicate that such an infinite series may be truncated after the third harmonic when pump power is not too strong.

Knowing that the nonlinear damping rate in steady state must equal to the initial growth rate. Γ_{s1}^N can be calculated from (6.2) and Figure 3,

however, this value is much smaller than the initial growth rate calculated from (4.17). We may conclude that there must exist another kind of non-linear damping mechanism which dominates in the saturation process.

It is well established that diffusion exists in a magnetically confined beam plasma, and usually pure coherent longitudinal modes does not cause an enhanced plasma loss across the magnetic field. With the plasma dimension smaller than the wavelength of the oscillation in question, magnetic field causes the charged particles to gyrate and move towards the side boundary to produce a field which causes the oscillating mode to become elliptically polarized. This induced field may cause an enhanced diffusion. While ordinary diffusion of electrons and ions across a magnetic field is caused by collisions with non-identical particles, it has been observed that certain oscillations seem to enable the plasma to acquire an enhanced diffusion rate. The behavior of a low temperature plasma is then largely governed by the diffusion processes³³ involved, but the anomalous diffusion can be visualized as a consequence of additional particle collision with the electric field of the oscillating instability. This can also be regarded as made of $\underline{E} \times \underline{B}$ drift motion of the particles, and most readily understood from the test - particle point of view. Let's write the equation of motion for a single ion moving in a wave field with the presence of a uniform magnetic field $B_0 \hat{z}$ as follows:

$$\frac{d\underline{r}}{dt} = \underline{v}$$

(6.3)

$$M \frac{d\underline{v}}{dt} = e \left\{ \underline{E}(\underline{r}(t), t) + \frac{1}{c} \underline{v} \times B_0 \right\} = e \underline{E}(\underline{r}(t), t) + M \Omega_i \underline{v}(\underline{r}(t), t) \times \hat{z}$$

and the solution of (6.3) may be expressed as

$$\underline{v}(\underline{r}(t), t) = \underline{R}_i(t) \cdot \underline{v}(0) + \frac{e}{M} \int_0^t dt' \underline{R}_i(t-t') \cdot \underline{E}(\underline{r}(t'), t') \quad (6.4)$$

$$\underline{r}(t) = \underline{r}(0) + \frac{1}{\Omega_i} \underline{L}_i(t) \cdot \underline{v}(0) + \frac{c}{B_0} \int_0^t dt' \underline{L}_i(t-t') \cdot \underline{E}(\underline{r}(t'), t')$$

where

$$\underline{R}_i(t) = \frac{1}{\Omega_i} \frac{d}{dt} \underline{L}_i(t) = \begin{bmatrix} \cos \Omega_i t & \sin \Omega_i t & 0 \\ -\sin \Omega_i t & \cos \Omega_i t & 0 \\ 0 & 0 & 1 \end{bmatrix} \quad \underline{L}_i(t) = \begin{bmatrix} \sin \Omega_i t & 1 - \cos \Omega_i t & 0 \\ -(1 - \cos \Omega_i t) & \sin \Omega_i t & 0 \\ 0 & 0 & \Omega_i t \end{bmatrix}$$

Thus the position $\underline{R}(t)$ of the guiding center is obtained as

$$\begin{aligned} \underline{R}(t) &= \underline{r}(t) - \frac{1}{\Omega_i} \hat{z} \times \underline{v}(t) \\ &= \underline{R}_0 - \frac{c}{B_0} \hat{z} \times \int_0^t dt' \underline{E}(\underline{r}(t') + \hat{z} \{v_{\parallel}(0)t + \frac{e}{M} \int_0^t dt'' E_{\parallel}(\underline{r}_i(t''), t'')\}) \end{aligned} \quad (6.5)$$

and the transverse drift velocity of the guiding center is given by

$$\underline{V}_{\perp}(\underline{r}(t), t) = \frac{d\underline{R}_{\perp}(t)}{dt} = - \frac{c}{B_0} \hat{z} \times \underline{E}(\underline{r}(t), t) \quad (6.6)$$

where

$$\underline{R}_{\perp}(t) = \underline{R}_{\perp 0} - \frac{c}{B_0} \hat{z} \times \int_0^t dt' \underline{E}(\underline{r}(t'), t') \quad (6.7)$$

with the aid of Eq. (6.5), $\underline{V}_{\perp}(\underline{r}(t), t)$ may be expanded with respect to the center position $\underline{R}(t)$ as

$$\begin{aligned} \underline{V}_{\perp}(\underline{r}(t), t) &= \underline{V}_{\perp}(\underline{R}(t), t) + \frac{1}{\Omega_i} \hat{z} \times \underline{v}(t) \cdot \nabla \underline{V}_{\perp}(\underline{R}(t), t) + \dots \\ &= - \frac{c}{B_0} \hat{z} \times \{ \underline{E}(\underline{R}(t), t) + \frac{1}{\Omega_i} \hat{z} \times \underline{v}(t) \cdot \nabla \underline{E}(\underline{R}(t), t) + \dots \} \end{aligned} \quad (6.8)$$

This would give the following relation immediately

$$\underline{V}_{\perp}(\underline{R}(t), t) = - \frac{c}{B_0} \hat{z} \times \underline{E}(\underline{R}(t), t) \quad (6.9)$$

where $\underline{R}_{\perp}(t)$ may be approximately expressed as

$$\underline{R}_{\perp}(t) = \underline{R}_{\perp 0} - \frac{c}{B_0} \hat{z} \times \int_0^t dt' \underline{E}(\underline{R}(t'), t') \quad (6.10)$$

therefore, in the Euler's coordinate system we have

$$\underline{V}_{\perp}(\underline{R}, t) = - \frac{c}{B_0} \hat{z} \times \underline{E}(\underline{R}, t) \quad (6.11)$$

and

$$V_x(\underline{R}, t) = \frac{c}{B_0} E_y(\underline{R}, t) \quad (6.12)$$

Due to the spatially dependent force field, there is a force difference between two different points, i. e., finite excursion of the oscillating ion brings itself into regions of different field intensity. The explicit expression for the statement above is given by

$$\frac{\partial}{\partial t} V_x(\underline{R}_2, t) - \frac{\partial}{\partial t} V_x(\underline{R}_1, t) = \delta \underline{R} \cdot \nabla \frac{\partial}{\partial t} V_x(\underline{R}_1, t) \quad (6.13)$$

where $\delta \underline{R} = \underline{R}_2 - \underline{R}_1$

now let's define a force due to the force difference

$$\frac{d}{dt} V_x^{(2)}(\underline{R}_1, t) = \langle \frac{\partial}{\partial t} V_x(\underline{R}_2, t) - \frac{\partial}{\partial t} V_x(\underline{R}_1, t) \rangle = \langle \delta \underline{R} \cdot \nabla \frac{\partial}{\partial t} V_x(\underline{R}_1, t) \rangle \quad (6.14)$$

where $\langle \rangle$ is meant to ensemble average

let

$$\delta \underline{R} = - \frac{c}{B_0} \hat{z} \times \int_0^t dt' \underline{E}(\underline{R}_1, t') + \hat{z} \{ v_{\parallel}(0)t + \frac{e}{M} \int_0^t dt' \int_0^{t'} dt'' E_{\parallel}(\underline{R}_1, t'') \} \quad (6.15)$$

and assume

$$E_y(\underline{R}_1, t) = A_y \cos k \cdot \underline{R}_1 \sin(\omega t + \phi) \quad (6.16)$$

where $\underline{k} = k\hat{x}$ and ϕ is a random phase which is a constant during the period of two successive collisions.

Substituting (6.15) and (6.16) in eq. (6.14), yields

$$\begin{aligned}
 \frac{d V_x^{(2)}(\underline{R}_1, t)}{dt} &= < -\frac{c^2}{B_o^2} k A_y^2 \left[\int_0^t dt' \cos(\underline{k} \cdot \underline{R}_1) \sin(\omega t' + \phi) \right] \sin(\underline{k} \cdot \underline{R}_1) \cos(\omega t + \phi) \omega > \\
 &= < \frac{c^2}{B_o^2} k A_y^2 \sin \underline{k} \cdot \underline{R}_1 \cos \underline{k} \cdot \underline{R}_1 [\cos(\omega t + \phi) - \cos \phi] \cos(\omega t + \phi) > \\
 &= \frac{c^2}{4B_o^2} k A_y^2 \sin 2 \underline{k} \cdot \underline{R}_1 (1 - \cos \omega t)
 \end{aligned} \tag{6.17}$$

therefore, the maximum contribution to $V_x^{(2)}(\underline{R}_1)$ between two successive collisions is

$$V_x^{(2)}(\underline{R}_1) = \frac{c^2}{4B_o^2} k A_y^2 \sin(2 \underline{k} \cdot \underline{R}_1) \tau_c \tag{6.18}$$

and with the assumption

$$\omega \gg \frac{1}{\tau_c} \tag{6.19}$$

where τ_c is the collision time.

Because of the spatial dependence of $V_x^{(2)}(\underline{R}_1)$, it will give an additional damping to $V_x(\underline{R}_1, t)$.

In fluid limit, \underline{R}_1 is not the initial position of the particle trajectory, it is an independent variable. Thus

$$\frac{\partial \underline{R}_1}{\partial t} = 0 \tag{6.20}$$

since

$$\frac{\partial}{\partial t} V_x(\underline{R}_1, t) + V_x(\underline{R}_1, t) \cdot \nabla [V_x(\underline{R}_1, t) + V_x^{(2)}(\underline{R}_1)] = \frac{c}{B_o} \frac{d}{dt} E_y(\underline{R}_1, t) - v_{in} V_x(\underline{R}_1, t) \tag{6.21}$$

This may be written as

$$\begin{aligned} \frac{\partial}{\partial t} V_x(\underline{R}_1, t) + V_x(\underline{R}_1, t) \cdot \nabla V_x(\underline{R}_1, t) &= \frac{c}{B_0} \frac{d}{dt} E_y(\underline{R}_1, t) - v_{in} V_x(\underline{R}_1, t) - \frac{c^2}{2B_0^2} k^2 A_y^2 \\ &\quad \cos(2\underline{k} \cdot \underline{R}_1) \tau_c V_x(\underline{R}_1, t) \\ &= \frac{c}{B_0} \frac{d}{dt} E_y(\underline{R}_1, t) - v_{eff} V_x(\underline{R}_1, t) \end{aligned} \quad (6.22)$$

where $v_{in} = \frac{1}{\tau_c}$,

and

$$v_{eff} = v_{in} + \frac{c^2}{2B_0^2} k^2 A_y^2 \cos(2\underline{k} \cdot \underline{R}_1) \tau_c \quad (6.23)$$

Hence at center, where $\underline{R}_1 = 0$ and

$$v_{eff} = v_{in} + \frac{c^2}{2B_0^2} k^2 A_y^2 / v_{in} \quad (6.24)$$

Assuming $A_y = \xi A$, where A is the amplitude of E_x and $0 \leq \xi \leq 1$,

the nonlinear damping rate Γ_{s2}^N of the electrostatic ion cyclotron wave due to the anomalous diffusion becomes

$$\Gamma_{s2}^N = \frac{c^2}{4B_0^2} k^2 \xi^2 A^2 / 2\Gamma_s \quad (6.25)$$

3. Comparison between Theory and Experimental Results

As mentioned in Chapter V, the nonlinear damping rate at steady state must equal the initial growth rate. From Figure 9 the initial growth rate $\gamma = 1.5 \times 10^5 / \text{sec}$ for $P_1 = 173$ watts is obtained. The amplitude of the potential oscillation for $P_1 = 173$ watts can be found in Figure 4. Since the amplitude of the potential oscillation is the integration of the amplitude of the field oscillation, then $A = 1.05 \times k = 3.5$ volts/cm is found.

First let's calculate the nonlinear damping rate due to the harmonic generation. From Figure 3 and Eq. (6.2), we find

$$\Gamma_{s1}^N = .32 \times 10^5 / \text{sec} \quad (6.26)$$

with the aid of Table 2 and Eq. (6.25), we have

$$\Gamma_{s2}^N = 10 \xi^2 \times 10^5 / \text{sec} \quad (6.27)$$

since

$$\Gamma_{s1}^N + \Gamma_{s2}^N = \gamma = 1.5 \times 10^5$$

we find

$$\xi = .34 \approx \frac{\Omega_i}{\omega_s} .$$

VII. CONCLUSIONS

The physical origin of mode coupling mechanism in an infinite plasma is described as electrostrictive effect. Based on this physical viewpoint, a general approach to analyze the parametric decay processes of plasma waves is presented. A set of coupled mode equations is derived by using Hamiltonian approach, and the coupling coefficients are derived from the collisionless Boltzman-Vlasov equation. The threshold for parametric amplification of an electrostatic ion cyclotron mode (longitudinal wave) and a harmonic of electron cyclotron mode (hybrid wave) in the presence of external radiation of an appropriate frequency has been found.

³⁴
An experiment is performed in a microwave sustained plasma. The properties of the process are in qualitative agreement with the theory. Saturation of the instability is also observed in the experiment, and the nonlinear mechanisms are found to be anomalous diffusion and harmonic generation, again, in agreement with the theoretical results.

APPENDIX A: NORMALIZATION OF THE ACOUSTIC MODES

The first step in the quantization procedure is to write down the Hamiltonian density. Let's define a lattice for a homogenous medium of mass density $\rho = n_o M$, where n_o and M are respectively the ion density and mass, then attach a dressed vibrating ion to each lattice point. Let the deviation of the m th ion's position from its equilibrium position x_m be given by q_m , we are led to write for the acoustic modes³⁵

$$H = \frac{1}{2} \sum_{m=1}^{n_o} \left[\frac{P_m^2}{M} + C_L (q_{m+1} - q_m)^2 \right] \quad (A.1)$$

Where for the $m=n_o$ term, $q_{n_o+1} = q_1$ because of the periodic boundary conditions and $P_m = M \dot{q}_m$, $x_m = m \left(\frac{1}{n_o} \right)^{\frac{1}{3}}$ and C_L is the force constant.

The first term in the brackets corresponds to the kinetic energy of the oscillating ions, the second to the potential energy associated with the Hooke's law force. We shall now proceed to rewrite H so that it has the same form as the Hamiltonian for the linear harmonic oscillator. Let us express the coordinates q_m and momenta P_m in terms of the traveling wave normal mode expansion

$$q_m^{(k)} = \left(\frac{1}{2n_o M \omega_k'} \right)^{\frac{1}{2}} (a_k e^{ik \cdot x_m}) \text{ and } q_m = \sum_k q_m^{(k)} \quad (A.2)$$

$$P_m^{(k)} = M \dot{q}_m^{(k)} = -i \left(\frac{M \omega_k'}{2n_o} \right)^{\frac{1}{2}} (a_k e^{ik \cdot x_m} - a_k^+ e^{-ik \cdot x_m}) \text{ and } P_m = \sum_k P_m^{(k)} \quad (A.3)$$

where we have $\dot{a}_k = -i \omega_k' a_k$ $\dot{a}_k^+ = i \omega_k' a_k^+$

$$\therefore \sum_{m=1}^{n_0} P_m^2 = \sum_{m=1}^{n_0} (-i) \sum_k \left(\frac{M\omega'_k}{2n_0} \right)^{\frac{1}{2}} (a_k e^{ik \cdot x_m} - a_k^+ e^{-ik \cdot x_m}) (-i) \sum_{k'} \left(\frac{M\omega'_{k'}}{2n_0} \right)^{\frac{1}{2}} (a_{k'} e^{ik' \cdot x_m}$$

$$- a_{k'}^+ e^{-ik' \cdot x_m}) = - \sum_k \frac{\omega'_k}{2} (a_k a_k + a_k a_k^+ - a_k^+ a_k + a_k^+ a_k^+) \quad (A.4)$$

$$\text{and } \sum_{m=1}^{n_0} (q_{m+1} - q_m)^2 = \sum_k \frac{\omega'_k}{2C_L} (a_k a_k + a_k a_k^+ + a_k^+ a_k + a_k^+ a_k^+) \quad (A.5)$$

$$\therefore H = \frac{1}{2} \sum_k \omega'_k (a_k a_k^+ + a_k^+ a_k) \quad (A.6)$$

If a_k and a_k^+ are now defined in terms of the new variables $Q^{(k)}$ and $K^{(k)}$ as follows:

$$a_k = \left(\frac{M}{2\omega'_k} \right)^{\frac{1}{2}} (\omega'_k Q^{(k)} + i \frac{K^{(k)}}{M}) \quad (A.7)$$

$$a_k^+ = \left(\frac{M}{2\omega'_k} \right)^{\frac{1}{2}} (\omega'_k Q^{(k)} - i \frac{K^{(k)}}{M}) \quad (A.8)$$

then above Hamiltonian reduces to the harmonic oscillator form

$$H = \frac{1}{2} \sum_k \left[\frac{K^{(k)2}}{M} + M \omega_k'^2 Q^{(k)2} \right] \quad (A.9)$$

With the Hamiltonian in the form above we proceed to quantize the acoustic vibrations by postulating that the $Q^{(k)}$, $K^{(k)}$ are operators that satisfy the poisson bracket relations $\{ Q^{(k)}, K^{(k')} \} = \delta_{kk'}$.

Now let us normalize the field produced by the acoustic vibrations

$$n_o e \delta E = e \sum_{m=1}^{n_o} \sum_k \delta E^{(k)} e^{ik \cdot x_m} = \sum_{m=1}^{n_o} \sum_k \dot{P}_m^{(k)} = - \sum_{k,m=1}^{n_o} \omega'_k \left(\frac{\omega'_k M}{2n_o} \right)^{\frac{1}{2}} (a_k e^{ik \cdot x_m} + a_k^\dagger e^{-ik \cdot x_m})$$

(A. 10)

$$\begin{aligned} \dots e^{-ik \cdot x_m} &= e^{-ik \cdot x_{m-n_o}} e^{ik \cdot x_{n_o-m}} \dots \sum_{m=1}^{n_o} e^{ik \cdot x_{n_o-m}} = \sum_{m=1}^{n_o} e^{ik \cdot x_m} \\ \dots e \sum_{m=1}^{n_o} \sum_k \delta E^{(k)} e^{ik \cdot x_m} &= - \sum_{k,m=1}^{n_o} \omega'_k \left(\frac{\omega'_k M}{2n_o} \right)^{\frac{1}{2}} (a_k + a_k^\dagger) e^{ik \cdot x_m} \\ &= - \sum_{k,m=1}^{n_o} \omega'_k \left(\frac{\omega'_k M}{2n_o} \right)^{\frac{1}{2}} (2M\omega'_k)^{\frac{1}{2}} Q^{(k)} e^{ik \cdot x_m} \end{aligned}$$

(A. 11)

$$\begin{aligned} &= - \sum_{k,m=1}^{n_o} \left(\frac{1}{n_o} \right)^{\frac{1}{2}} M \omega_k'^2 Q^{(k)} e^{ik \cdot x_m} \\ \therefore \delta E^{(k)} &= - \frac{M}{e} \frac{1}{\sqrt{n_o}} \omega_k'^2 Q^{(k)} \end{aligned}$$

(A. 12)

Where ω'_k is the resonant frequency of the medium without pump field. If the pump field presents in the medium and near threshold level or above, the resonant frequency will shift to undamped frequency ω_k , in this case we can keep the unperturbed Hamiltonian H_o as before, but change ω'_k to ω_k for the relation between $\delta E^{(k)}$ and $Q^{(k)}$.

$$\therefore H_o^{(k)} = \frac{1}{2} \left[\frac{K^{(k)^2}}{M} + M \omega_k^2 Q^{(k)^2} \right]$$

(A. 13)

$$\delta E^{(k)} = - \frac{M}{e} \frac{1}{\sqrt{n_o}} \omega_k^2 Q^{(k)}$$

(A. 14)

It is easy to be generalized to three - dimensional case

$$\therefore H_o^{(k)} = \frac{1}{2} \sum_{\sigma} \left[\frac{K_{\sigma}^{(k)^2}}{M} + M \omega_k^2 Q_{\sigma}^{(k)^2} \right] \quad (A.15)$$

$$\delta \underline{E}^{(k)} = - \frac{M}{e} \frac{1}{\sqrt{n_o}} \omega_k^2 \underline{Q}^{(k)} \quad (A.16)$$

We can also generalize above procedure to an anisotropic case, for example, if there is a uniform magnetic field B_o in the z direction

$$\therefore H_o^{(k)} = \frac{1}{2} \sum_{\sigma} \left[\frac{K_{\sigma}^{(k)^2}}{M} + M \omega_k^2 Q_{\sigma}^{(k)^2} \right] \quad (A.17)$$

$$\delta \underline{E}^{(k)} = - \frac{M \omega_k^2}{\sqrt{n_o} e} \underline{Q}^{(k)} - \frac{\Omega_i}{e \sqrt{n_o}} \underline{K}^{(k)} \times \hat{z} \quad (A.18)$$

where we have $\{ Q_{\sigma}^{(k)}, K_{\beta}^{(k')} \} = \delta_{kk'} \delta_{\sigma\beta}$ and $\Omega_i = \frac{e B_o}{Mc}$

APPENDIX B: NORMALIZATION OF THE OPTICAL MODES

Because of the big difference between the masses of electron and ion, ion cannot follow the high frequency electron oscillation, hence we can consider this kind oscillations are optical modes in which electrons and ions vibrate against one another. Let's expand the displacements of the individual electrons in terms of the normal coordinates U^k and A_k, A_k^+

$$ie \delta y_i = \frac{1}{\sqrt{n_o}} \sum_k U^{(k)} e^{ik \cdot y_i} = \sum_k \left(\frac{1}{2n_o m \Omega'_k} \right)^{\frac{1}{2}} (A_k e^{ik \cdot y_i} + A_k^+ e^{-ik \cdot y_i}) \quad (B.1)$$

In terms of these normal coordinates we may write the total energy at any time

$$\mathcal{E}_{tot} = \sum_i \left[\frac{m}{2} (\delta \dot{y}_i)^2 + \frac{C_1}{2} (\delta y_i)^2 \right] \quad (B.2)$$

$$\therefore H = \frac{1}{2} \sum_k \Omega'_k (A_k A_k^+ + A_k^+ A_k) \quad (B.3)$$

where we have $\dot{A}_k = -i \Omega'_k A_k$, $\dot{A}_k^+ = i \Omega'_k A_k^+$

$$\begin{aligned} \therefore \frac{1}{\sqrt{n_o}} \sum_{i=1}^{n_o} \sum_k U^{(k)} e^{ik \cdot y_i} &= \sum_k \sum_{i=1}^{n_o} \left(\frac{i}{2n_o m \Omega'_k} \right)^{\frac{1}{2}} (A_k e^{ik \cdot y_i} + A_k^+ e^{-ik \cdot y_i}) \\ &= \sum_k \sum_{i=1}^{n_o} \left(\frac{1}{2n_o m \Omega'_k} \right)^{\frac{1}{2}} (A_k e^{ik \cdot y_i} + A_k^+ e^{-ik \cdot y_{i-n}}) \\ &= \sum_k \sum_{i=1}^{n_o} \left(\frac{1}{2n_o m \Omega'_k} \right)^{\frac{1}{2}} (A_k e^{ik \cdot y_i} + A_k^+ e^{ik \cdot y_{n-i}}) \\ &= \sum_k \sum_{i=1}^{n_o} \left(\frac{1}{2n_o m \Omega'_k} \right)^{\frac{1}{2}} (A_k + A_k^+) e^{ik \cdot y_i} \end{aligned} \quad (B.4)$$

$$\Rightarrow U^{(k)} = \left(\frac{1}{2m\Omega'_k} \right)^{\frac{1}{2}} (A_k + A_k^+) \quad (B.5)$$

$$\therefore \mathcal{H}^{(k)} = m \dot{U}^{(k)} = -i \left(\frac{m\Omega'_k}{2} \right)^{\frac{1}{2}} (A_k - A_k^+) \quad (B.6)$$

$$\therefore A_k A_k^+ = \frac{m}{2\Omega'_k} (\Omega'_k{}^2 U^{(k)2} - i \frac{\Omega'_k}{m} U^{(k)} \mathcal{H}^{(k)} + i \frac{\Omega'_k}{m} \mathcal{H}^{(k)} U^{(k)} + \frac{\mathcal{H}^{(k)2}}{m^2})$$

$$A_k^+ A_k = \frac{m}{2\Omega'_k} (\Omega'_k{}^2 U^{(k)2} + i \frac{\Omega'_k}{m} U^{(k)} \mathcal{H}^{(k)} - i \frac{\Omega'_k}{m} \mathcal{H}^{(k)} U^{(k)} + \frac{\mathcal{H}^{(k)2}}{m^2})$$

$$\therefore H = \frac{1}{2} \sum_k \left[\frac{\mathcal{H}^{(k)2}}{m} + m \Omega'_k{}^2 U^{(k)2} \right] \quad (B.7)$$

Now that we have obtained the Hamiltonian classically we may move directly to canonical operator form. Then $\mathcal{H}^{(k)}$ and $U^{(k)}$ become canonical variables satisfy the Poisson bracket relation

$$\{ U^{(k)}, \mathcal{H}^{(k')} \} = \delta_{kk'}$$

The final stage is to normalize the field produced by the optical vibrations

$$-en_o \delta \underline{E} = -e \sum_{i=1}^{n_o} \sum_k \delta E^{(k)} e^{i \underline{k} \cdot \underline{Y}_i} = \sum_{i=1}^{n_o} \sum_k -m \Omega'_k{}^2 \frac{1}{\sqrt{n_o}} U^{(k)} e^{i \underline{k} \cdot \underline{Y}_i}$$

$$\therefore \delta E^{(k)} = \frac{1}{\sqrt{n_o}} \frac{m \Omega'_k{}^2}{e} U^{(k)} \quad (B.8)$$

For the same reason, if pump field is present and near or above the threshold level

$$\therefore H_o^{(k)} = \frac{1}{2} \left[\frac{\mathcal{H}^{(k)2}}{m} + m \Omega'_k{}^2 U^{(k)2} \right] \quad (B.9)$$

$$\delta E^{(k)} = \frac{1}{\sqrt{n_0}} \frac{m \Omega_k^2}{e} U^{(k)} \quad (B.10)$$

In three dimensional case we have

$$H_0^{(k)} = \frac{1}{2} \sum_{\sigma} \left[\frac{\mathcal{H}_{\sigma}^{(k)^2}}{m} + m \Omega_k'^2 U_{\sigma}^{(k)^2} \right] \quad (B.11)$$

$$\delta \underline{E}^{(k)} = \frac{1}{\sqrt{n_0}} \frac{m \Omega_k^2}{e} \underline{U}^{(k)} \quad (B.12)$$

We can also generalized above procedure to the case that there is an uniform magnetic field B_0 in the \hat{z} direction

$$H_0^{(k)} = \frac{1}{2} \sum_{\sigma} \left[\frac{\mathcal{H}_{\sigma}^{(k)^2}}{m} + m \Omega_k'^2 U_{\sigma}^{(k)^2} \right] \quad (B.13)$$

$$\delta \underline{E}^{(k)} = \frac{m \Omega_k^2}{e \sqrt{n_0}} \underline{U}^{(k)} + \frac{\Omega_e}{e \sqrt{n_0}} \underline{\mathcal{H}}^{(k)} \times \hat{z} \quad (B.14)$$

where $\Omega_e = \frac{-e B_0}{m_e c}$ $\{ U_{\sigma}^{(k)}, \mathcal{H}_{\beta}^{(k')} \} = \delta_{kk'} \delta_{\sigma\beta}$

REFERENCES

1. H.E. Carlson, W.E. Gordon, and R.L. Showen, J. Geophys. Res. 77, 1242 (1972); R.B. White, C.S. Liu and M.N. Rosenbluth, Phys. Rev. Lett. 31, 520 (1973); H.W. Hendel and J.T. Flick, Phys. Rev. Lett. 31, 199 (1973).
2. B. Grek and M. Porkolab, Phys. Rev. Letters 30 (1973) 836.
3. L.A. Klein and B.R. Cheo, Technical Report 402-12, 1973, N.Y. Univ.
4. M. Porkolab, V. Arunasalam, N.C. Luhmann, Jr. and J.P.M Schmitt, PPPL Report MATT-1160 (1975) .
5. M. Okabayashi, K. Chen and M. Porkolab, Phys. Rev. Letters 31 (1973) 1113.
6. V.I. Farenik, V.V. Vlasov and A.M. Rozhkov, Zh. Pis. Red. 18 (1973) 409. (Sov. Phys. JETP Lett. 18 (1973) 240) .
7. R.P.H. Chang and M. Porkolab, Phys. Rev. Letters 31 (1974) 1227; 31 (1973) 1241 .
8. M. Brusati, G. Cima, M. Fontanesi and E. Sindoni, Lettere al Nuovo Cimento 10 (1974) 67 .
9. V.P. Silin, Sov. Phys. JETP 21 (1965) 1127.
10. D.F. DuBois and M.V. Goldman, Phys. Rev. Letters 14 (1965) 544; Phys. Rev. 164 (1967) 207.
11. K. Nishikawa, J. Phys. Soc. Japan 24 (1968) 916, 1152.
12. Y.C. Lee and C.H. Su, Phys, Rev. 152 (1966) 129.
13. E.A. Jackson, Phys. Rev. 153 (1967) 203.
14. Y.M. Aliev, V.P. Silin and C. Watson, Sov. Phys. JETP 23 (1966) 626 .
15. T. Amano and M. Okamoto, J. Phys. Soc. Japan 26 (1969) 391.
16. M. Porkolab, Nuclear Fusion 12 (1972) 329.
17. M. Porkolab, Phys. Fluids 17 (1974) 1432.
18. R.Z. Sagdeev and A.A. Galeev, Nonlinear Plasma Theory, Chap. 1 (W.A. Benjamin, Inc. New York, 1969) .
19. S. Ichimaru, Basic Principles of Plasma Physics (W.A. Benjamin, Inc. 1973) .
20. R. Stenzel and A.Y. Wong, Phys. Rev. Letters 31 (1972) 274 .

21. M. Porkolab, Physica 82C (1976) 86-110 .
22. S. Hiroe and H. Ikegami, Phys. Rev. Letters 19 (1967) 1414 .
23. R.A. Stern and N. Tzoar, Phys. Rev. Letters 17 (1966) 903 .
24. L.A. Klein, B. Ru-Shao Cheo and R.A. Stern, J. Applied Phys., 45 (1974) 5218 .
L.A. Klein and B.R. Cheo , Technical Report 402-12, 1973 New York University .
25. K. Chung, K.C. Huang, and E. Oevi, Phys. Fluids 16 (1973) 1245.
26. R. Kristal, Ph.D. dissertation, June 1973, PINY .
27. V.V. Pustovalov and V.P. Silm, Sov. Phys. JETP 32 (1971) 1198 .
28. D.F. DuBois and M.V. Goldman, Phys. Fluids 15 (1972) 919 .
29. E. Valee, C. Oberman and F.W. Perking, Phys. Rev. Letters 28 (1972) 340.
30. J.A. Fejer and Y.Y. Kuo, Phys. Rev. Letters 29 (1972) 1667.
31. D.F. DuBois, M.V. Goldman and D. McKinnis, Fluids 16 (1974) 2257.
32. N. Bezzerides and J. Weinstock, Phys. Rev. Letters 28 (1972) 481
J. Weinstock and N. Bezzerides, Phys. Fluids 16 (1973) 2287; Phys. Rev. Letters 32 (1974) 754 .
33. F.C. Hoh, Rev. Modern Phys. 34 (1962) 267.
34. Experimental set up has been described in detail in Polytechnic Institute of N.Y. Technical Report, No. 77-028, 1977 by Q.T. Yip and B.R. Cheo.
35. R.H. Pantell and H.E. Puthoff, Fundamentals of Quantum Electronics, Chap. 7, John Wiley and Sons, Inc.
36. W.A. Harrison, Solid State Theory, Chap. 4, International Series in Pure and Applied Physics.

REPORT DOCUMENTATION PAGE		READ INSTRUCTIONS BEFORE COMPLETING FORM
1. REPORT NUMBER 18 AFOSR-TR-78-0033 ✓	2. GOVT ACCESSION NO.	3. RECIPIENT'S CATALOG NUMBER
4. TITLE (and Subtitle) STUDIES OF PARAMETRIC DECAY INSTABILITIES IN MAGNETO PLASMAS.	5. TYPE OF REPORT & PERIOD COVERED Final Scientific Report. Apr 1974 to June 1977.	
7. AUTHOR(s) Szu-Ping/Kuo and Bernard R-S/Cheo	6. PERFORMING ORG. REPORT NUMBER POLY-EE/EP-77-027 ✓	
9. PERFORMING ORGANIZATION NAME AND ADDRESS Polytechnic Institute of New York, EE Department 333 Jay Street Brooklyn, NY 11201	8. CONTRACT OR GRANT NUMBER(s) 15 AFOSR-74-2668 ✓	
11. CONTROLLING OFFICE NAME AND ADDRESS Air Force Office of Scientific Research / NP Bolling Air Force Base, Bldg. #410 Washington, DC 20332	10. PROGRAM ELEMENT, PROJECT, TASK AREA & WORK UNIT NUMBERS 16 9751-03 61102F	
14. MONITORING AGENCY NAME & ADDRESS (if different from Controlling Office)	12. REPORT DATE 11 June 1977	
	13. NUMBER OF PAGES 84 12 94 P.	
	15. SECURITY CLASS. (of this report) Unclassified	
15a. DECLASSIFICATION/DOWNGRADING SCHEDULE		
16. DISTRIBUTION STATEMENT (of this Report) Approved for public release, distribution unlimited		
17. DISTRIBUTION STATEMENT (of the abstract entered in Block 20, if different from Report)		
18. SUPPLEMENTARY NOTES		
19. KEY WORDS (Continue on reverse side if necessary and identify by block number) Plasmas Plasma Instabilities Non-Linear Study in Plasma Parametric Decay Instabilities		
20. ABSTRACT (Continue on reverse side if necessary and identify by block number) → A theory is developed for the parametric excitation of coupled waves in a uniform magneto plasma. Instead of using electrostatic approximation which is valid only for longitudinal waves, a general formulation of the parametric coupling equations is developed by using Hamiltonian approach. →		

→ The plasma is pumped by a monochromatic electromagnetic wave with frequency ω_0 which decays into two decay waves ω_1 and ω_s (e. g., a plasmon and a phonon), with $\omega_0 = \omega_1 + \omega_s$. Either one of the plasma modes coupled with the pump wave (through the linearized Vlasov equation) to induce a polarization which may act as the source of another mode. A general procedure to calculate the induced polarizations is introduced by transforming the linearized Vlasov equation into the oscillating frame of reference, in which the equation can then be solved by the method of characteristics. The threshold power, initial growth rate and the frequency shift (due to finite initial growth rate) of the parametric instabilities can be obtained from the coupled mode equations and the results obtained can be applied to all the wavelength region. Several interesting cases are presented and compared favorably with experiments.

The simultaneous excitation of second harmonic of electron-cyclotron and electrostatic ion-cyclotron oscillations by means of a monochromatic electromagnetic wave at $\omega_0 = 9.23$ GHz has been observed experimentally. The experiment has been conducted in a microwave sustained beam plasma. By switching the pump power between two levels, the time evolution of the excited electrostatic ion-cyclotron wave is studied. In order to explain the observed nonlinear saturated state of the instability, the nonlinear damping rate due to two possible mechanisms has been examined. Harmonic generation gives very small contributions, therefore, anomalous diffusion caused by the coherent oscillation of the electrostatic ion-cyclotron wave plays an important role. Working in the guiding center frame, the effective nonlinear damping frequency pertaining to the diffusion process is obtained.